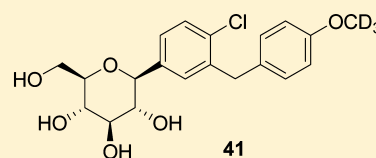


Design, Synthesis, and Biological Evaluation of Deuterated C-Aryl Glycoside as a Potent and Long-Acting Renal Sodium-Dependent Glucose Cotransporter 2 Inhibitor for the Treatment of Type 2 Diabetes

Ge Xu,^{†,‡} Binhua Lv,[‡] Jacques Y. Roberge,[‡] Baihua Xu,[‡] Jiyan Du,[‡] Jiajia Dong,[‡] Yuanwei Chen,[‡] Kun Peng,[‡] Lili Zhang,[‡] Xinxing Tang,[‡] Yan Feng,[‡] Min Xu,[‡] Wei Fu,[†] Wenbin Zhang,[‡] Liangcheng Zhu,[‡] Zhongping Deng,[‡] Zelin Sheng,[‡] Ajith Welihinda,[§] and Xun Sun^{*,†}[†]School of Pharmacy, Fudan University, 826 Zhangheng Road, Pudong New Area, Shanghai 201203, P. R. China[‡]Egret Pharma (Shanghai) Co., Ltd, 4F, 1118 Halei Road, Zhangjiang Hi-Tech Park, Pudong New Area, Shanghai 201203, P. R. China[§]Theracos Inc., 550 Del Rey Avenue, Sunnyvale, California 94805-3528, United States

Supporting Information

ABSTRACT: SGLT2 inhibitors deuterated at sites susceptible to oxidative metabolism were found to have a slightly longer t_{\max} and half-life ($t_{1/2}$), dose-dependent increase in urinary glucose excretion (UGE) in rats, and slightly superior effects on UGE in dogs while retaining similar in vitro inhibitory activities against *h*SGLT2. In particular, deuterated compound **41** has the potential to be a robust long-acting antidiabetic agent.



IC_{50} (*h*SGLT2) = 2.5 nM vs 3.2 nM (dapagliflozin)
UGE in dog (0–24 h) = 14682 mg vs 11610 mg (dapagliflozin)
 $t_{1/2}$ in rat = 6.3 h vs 4.5 h (dapagliflozin)
87% remaining parent compound **41** vs 43% remaining dapagliflozin

INTRODUCTION

Diabetes has increasingly become a burden on the world's population. In 2011, the WHO announced that 347 million people worldwide have diabetes, that an estimated 3.4 million people died from the complications of high blood sugar in 2004, and that diabetes deaths would double from 2005 to 2030.¹ Whereas type 1 diabetes is characterized by deficient insulin production, type 2 diabetes mellitus (DM2) is a complex disorder in which the interaction between environmental and genetic factors results in the development of insulin resistance (IR) and β -cell dysfunction.^{2,3} Oral medications for DM2 include metformin,⁴ alpha-glucosidase inhibitors,⁵ sulfonylureas,⁶ glinides,⁷ thiazolidinediones,^{8,9} and DPP-4 inhibitors.^{10,11}

Sodium-dependent glucose cotransporters (SGLTs) rely on the electrochemical potential of sodium ions to transport extracellular glucose actively into the cytoplasm. SGLT2 is a low-affinity, high-capacity transporter located almost exclusively on the apical surface of renal epithelial cells, whereas SGLT1 is expressed not only in the kidney but also in the intestine and other tissues. Approximately 90% of filtered glucose is reabsorbed by SGLT2 in the early proximal convoluted tubule (S1 and S2 segments) in mice, and the rest is reabsorbed by SGLT1 in the late proximal straight tubule (S3 segment), although in the absence of SGLT2, SGLT1 appears to be capable of reabsorbing approximately 70% of filtered glucose.^{12–15} By promoting urinary glucose excretion (UGE), SGLT2 inhibitors

allow treatment of DM2 by an insulin-independent mechanism that does not exacerbate the root cause, excess fat, implicated in the etiology of most cases of the disease. Because the natural O-aryl glycoside phlorizin (**1**) is a fairly potent SGLT2 inhibitor (Figure 1),^{16,17} early drug discovery efforts on SGLT2 inhibitors focused on O-aryl glycosides related to phlorizin, such as T-1095 (**2**),^{18,19} sergliflozin (**3**),²⁰ and remogliflozin (**4**),²¹ with the aim of increasing potency toward SGLT2 and minimizing activity toward SGLT1. Unfortunately, because of their susceptibility to the action of glycosidases and the ensuing poor pharmacokinetics, development of most O-aryl glycosides has ceased. The advent of C-aryl glycoside SGLT2 inhibitors, such as dapagliflozin (**5**, Bristol-Myers Squibb and AstraZeneca, approved by EMA in 2012),²² canagliflozin (**6**, Johnson & Johnson/Mitsubishi Tanabe, approved by FDA in 2013),²³ ipragliflozin (ASP1941, **7**, Astellas, phase III),²⁴ sotagliflozin (LX4211, **8**, Lexicon, phase II),²⁵ ertugliflozin (PF-04971729, **9**, Pfizer, phase II),²⁶ and EGT0001442 (**10**, Theracos, phase II),^{27,28} circumvented the problem of glycosidase susceptibility by removing the glycoside anomeric oxygen (Figure 2).

Compound **5** was reported to display a favorable absorption, distribution, metabolism, and excretion (ADME) profile in rats and humans and to control the blood glucose level well.²²

Received: August 13, 2013

Published: January 23, 2014

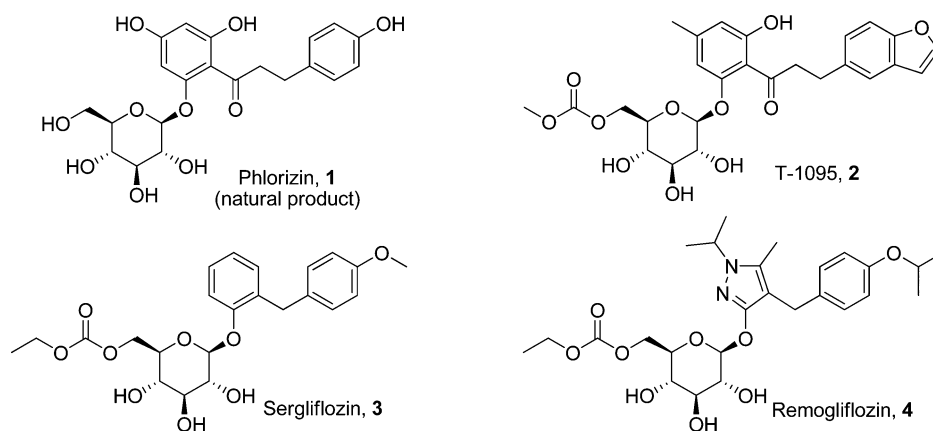


Figure 1. O-Aryl glycoside SGLT2 inhibitors.

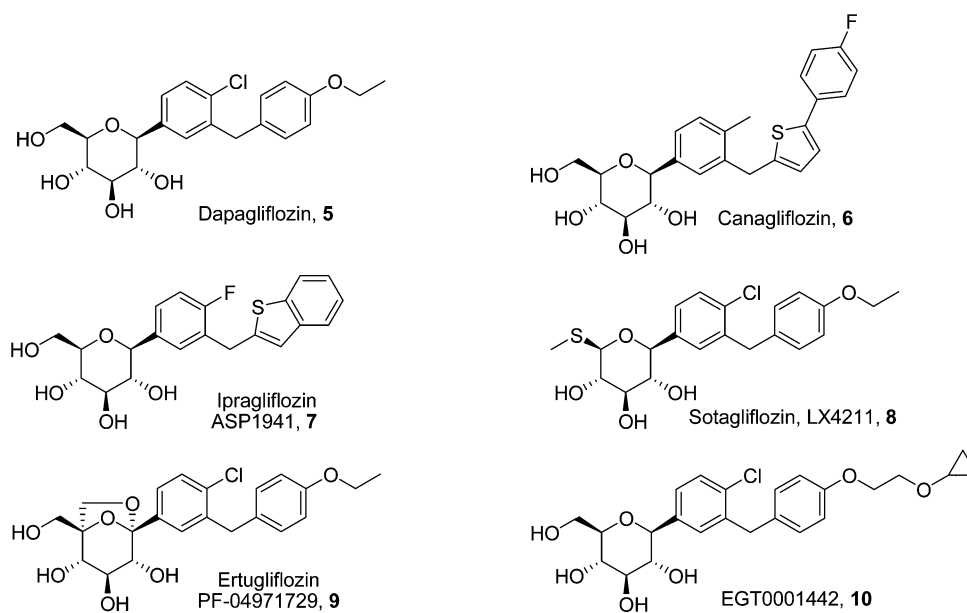


Figure 2. C-Aryl glycoside SGLT2 inhibitors.

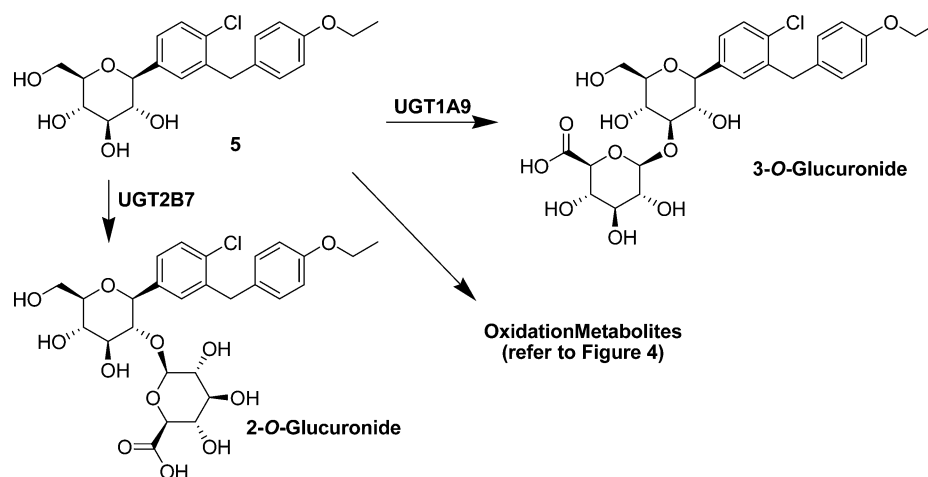


Figure 3. Metabolites of 5.

However, safety concerns²⁹ led an advisory committee to vote against the approval of 5 in January 2012, and drug approval in the United States was delayed even though it was approved in Europe in November 2012.

The toxicity of a drug could arise because of its unique chemical structure, its pharmacokinetics and tissue distribution, and/or the presence of toxic metabolites.³⁰ It was previously reported that excess quinones and methine-quinones might

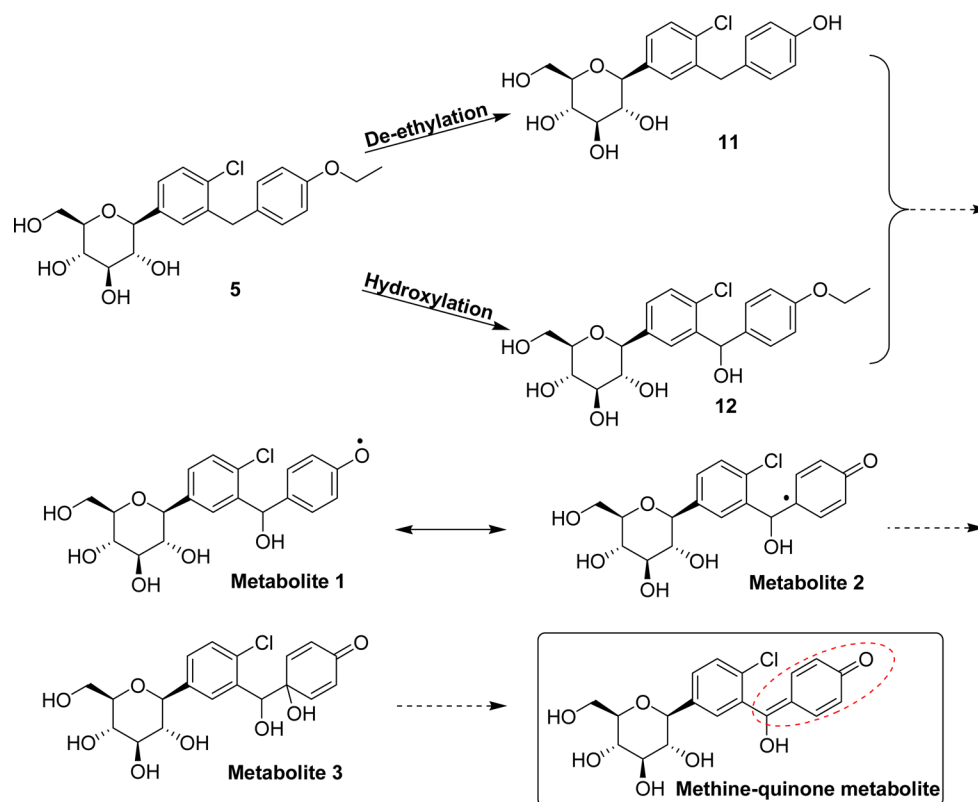


Figure 4. Proposed mechanism of formation of the putative methine-quinone metabolite from 5.

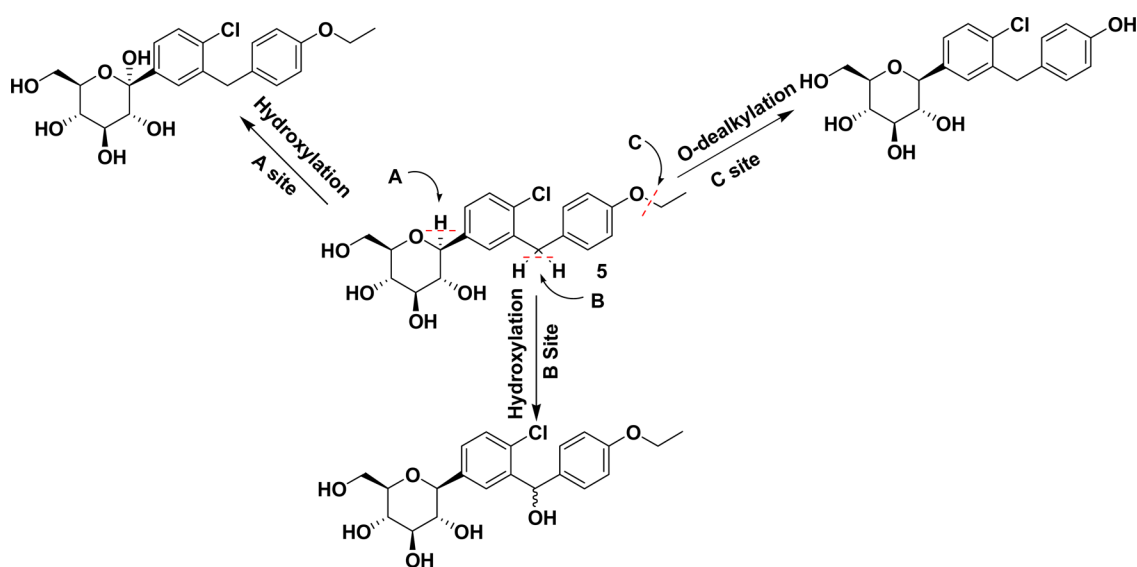


Figure 5. Predicted metabolic sites (A–C) of 5.

cause toxicities (e.g., hepatotoxicity).^{31,32} Benz et al. reported several novel pathways associated with quinone-induced stress in breast cancer cells.³³ It is also known that 5 is extensively metabolized via three main oxidative metabolic pathways in addition to extensive formation of glucuronides (Figure 3), and only low levels of the unchanged parent drug are excreted in the urine or feces³⁴ (main oxidative metabolites 11 and 12 are shown in Figure 4).³⁵ Therefore, after analysis of the structures of 5 and its main metabolites, 11 and 12, we hypothesized that 5 might eventually be converted into a methine-quinone derivative via 11 and/or 12 in vivo, which might be associated with possible

adverse events (Figure 4). Thus, we have attempted to block the potential metabolic hotspots on 5 and its close structural analogue 13 to increase their metabolic stability in vivo and to prevent or reduce the possibility of forming methine-quinone metabolites. As expected, compound 41 showed a much higher metabolic stability in vivo than 5 and was demonstrated to be a selective and long-acting SGLT2 inhibitor.

DESIGN

Replacing a hydrogen atom with fluorine has been extensively used to block metabolic hotspots. Recently, a renewed interest in

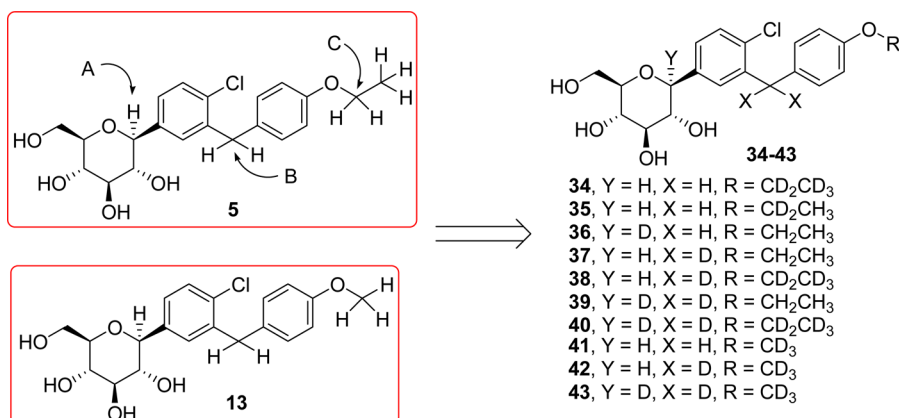
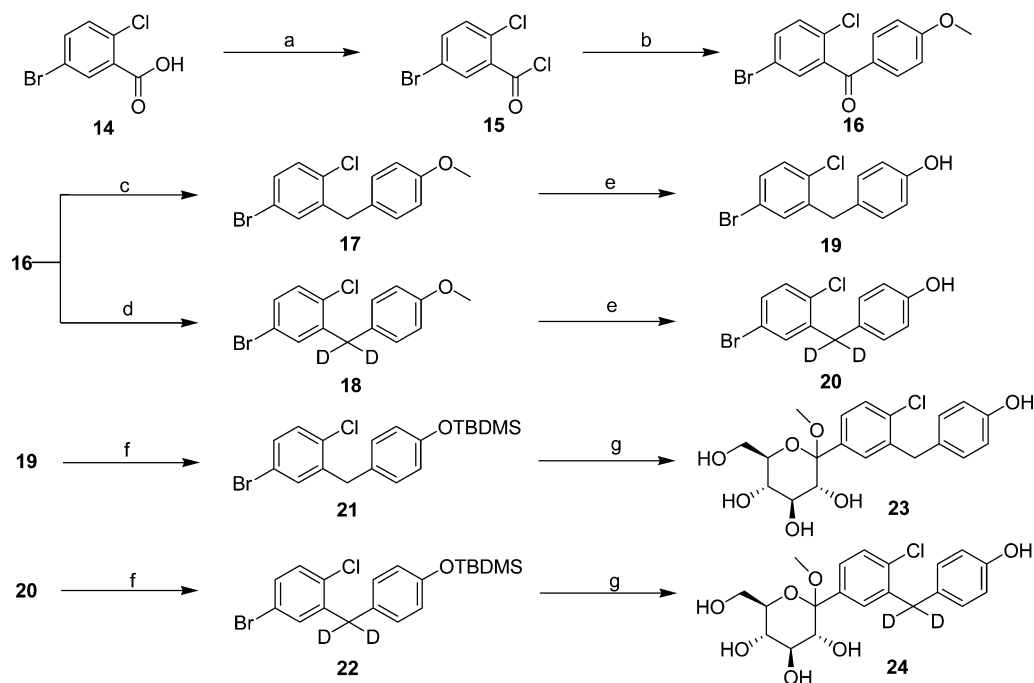


Figure 6. Deuteration strategy.

Scheme 1. Synthesis of 23 and 24^a

^aReagents and conditions: (a) (COCl)₂, CH₂Cl₂, DMF (cat.), 5–10 °C; (b) anisole, AlCl₃, CH₂Cl₂, –10 to 0 °C; (c) AlCl₃, NaBH₄, THF, 70 °C; (d) AlCl₃, NaBD₄, THF, 70 °C; (e) BBr₃, CH₂Cl₂, –20 to 0 °C; (f) *tert*-butylchlorodimethylsilane, triethylamine, acetonitrile, 0 to 5 °C; (g) *n*-BuLi, THF, PhCH₃, –78 °C, then 2,3,4,6-tetra-*O*-trimethylsilyl-β-D-gluconolactone followed by MeOH and concentrated hydrochloric acid.

the use of deuterium has also been used to serve a similar purpose.³⁶ By blocking a metabolic hotspot with deuterium, it is expected to not only reduce metabolite formation but also to improve the pharmacokinetic properties of drug candidates. Clinical studies with deuterated analogues of some known drugs have been initiated.^{36–40} Because of the isotope effect, the rate of C–D bond cleavage could be up to 10 times slower than cleavage of the C–H bond, making the deuterium analogue more resistant to chemical or enzymatic cleavage.⁴¹

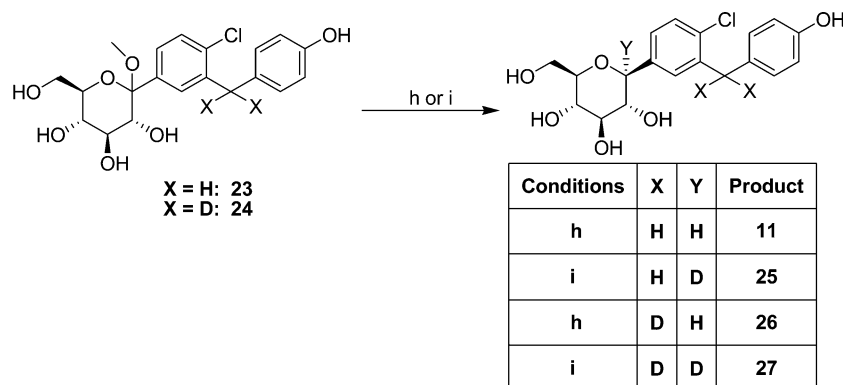
On the basis of the structure of **5**, we believed that it would go through oxidative metabolic transformation principally at three distinct sites (A–C, Figure 5): methine-C5 (A site) on the glycoside, leading to alpha hydroxylation, C13 in diarylmethane (B site), leading to hydroxylation, and O6 (C site), leading to dealkylation. Potential metabolic sites B and C were also confirmed by a later report on **5**.³⁵ Our efforts were therefore devoted to the design and synthesis of novel SGLT2 inhibitors

with a deuterium atom at the potential metabolic sites on **5** and its analogue **13** whose metabolism at these sites presumably could lead to the formation of methine-quinone metabolites. Figure 6 depicts the deuterated analogues that were pursued in the current study.

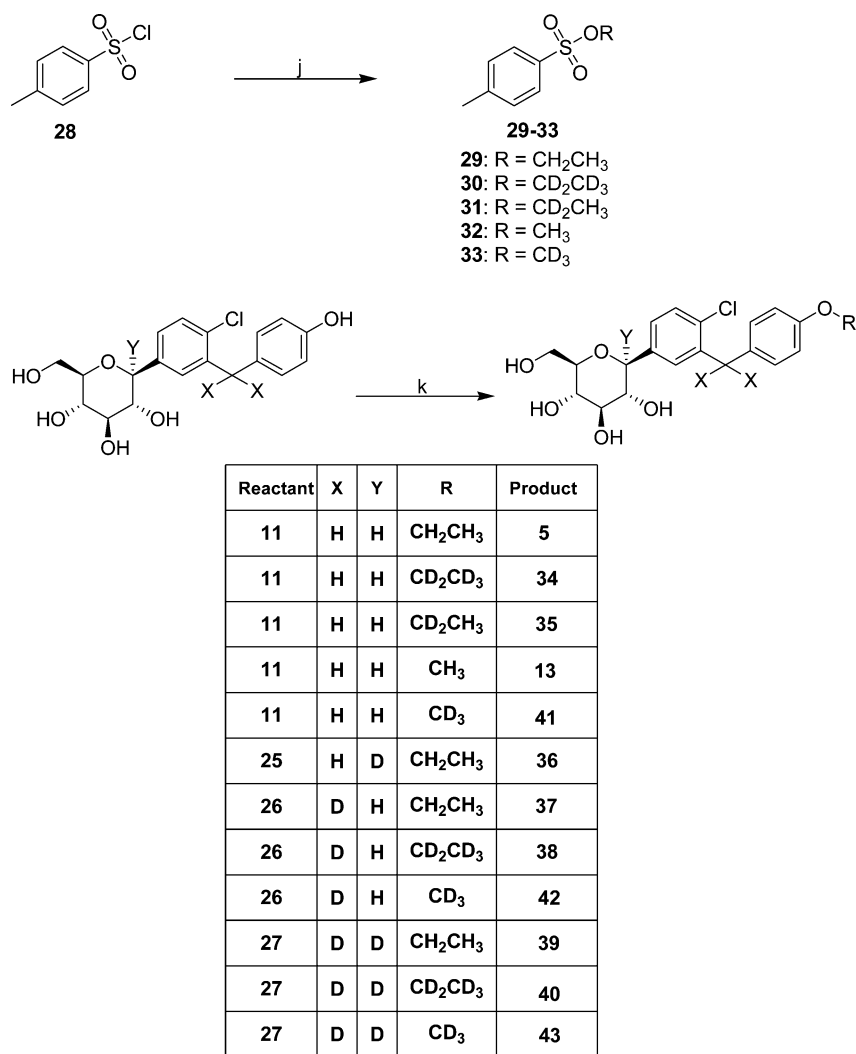
CHEMISTRY

The designed deuterated analogues **34–43** together with their parent compounds **5** and **13** (depicted in Figure 6) were prepared according to Schemes 1–3.

The synthesis of key intermediates **23** and **24** commenced from commercially available 5-bromo-2-chlorobenzoic acid (**14**), as illustrated in Scheme 1. **14** was first transformed into **15** via reaction with oxalyl chloride followed by a Friedel–Crafts acylation reaction using anisole and aluminum chloride, giving **16** in 83% yield after one crystallization from ethanol.²² Starting from **16**, after reduction (to **17** and **18**), demethylation (to **19**

Scheme 2. Synthesis of 11 and 25–27^a

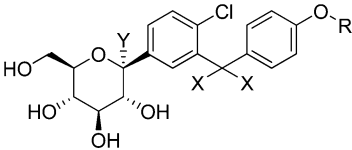
^aReagents and conditions: (h) Et₃SiH, BF₃·OEt₂, CH₂Cl₂, CH₃CN, –20 to –10 °C; (i) Et₃SiD, BF₃·OEt₂, CH₂Cl₂, CH₃CN, –20 to –10 °C.

Scheme 3. Synthesis of 29–33, 5, 13, and 34–43^a

^aReagents and conditions: (j) 4.6 N aqueous NaOH, ROH, THF, –5 to 15 °C; (k) TsOR (29–33), Cs₂CO₃, DMF, 40 °C.

and 20), protection with *tert*-butyldimethylsilyl (TBDMS) (to 21 and 22), and a final coupling with D-gluconolactone, 23 and 24 were obtained. Reduction of 16 with sodium borohydride and aluminum chloride in THF provided 17 in 95% yield, and using sodium borodeuteride and aluminum chloride in THF under refluxing conditions, 18 was obtained from 16 in 95% yield and

with 98% deuterium incorporation,⁴² thus leading to a nearly complete deuteration at the B site. It should be pointed out that we have also tried to use the following two treatments to achieve the transformation of 16 to 17 (or 18) on a small scale, but they were not used in the current study because of the high cost of deuterated triethylsilane (Et₃SiD) with boron trifluoride etherate

Table 1. In Vitro hSGLT Inhibitory Activity and Selectivity^a


compound	Y	X	R	hSGLT2 IC ₅₀ (nM)	hSGLT1 IC ₅₀ (nM)	hSGLT1/hSGLT2 selectivity
5 ⁵⁴	H	H	CH ₂ CH ₃	3.2	3140	981
34	H	H	CD ₂ CD ₃	2.5	3170	1268
35	H	H	CD ₂ CH ₃	7.5	>10 000	>1333
36	D	H	CH ₂ CH ₃	2.9	3060	1055
37	H	D	CH ₂ CH ₃	3.2	3988	1246
38	H	D	CD ₂ CD ₃	7.5	5040	672
39	D	D	CH ₂ CH ₃	6.5	>10 000	>1538
40	D	D	CD ₂ CD ₃	7.2	>10 000	>1388
13	H	H	CH ₃	1.9	540	284
41	H	H	CD ₃	2.5	900	360
42	H	D	CD ₃	0.8	820	1025
43	D	D	CD ₃	6.8	7000	1029

^aIC₅₀ values for SGLT1 and SGLT2 activities were obtained using eight-point dose-response curves constructed from triplicate measurements.

Table 2. Pharmacokinetic Parameters after Oral Compound Administration to SD Rats^a

compound	dose (mg/kg)	PK in rat			
		t _{max} (h)	C _{max} (ng/mL)	AUC _{0-∞} (ng h/mL)	t _{1/2} (h)
5	3	0.88 ± 0.75	1603 ± 425	11 658 ± 2918	4.52 ± 0.98
34	3	1.38 ± 0.75	2285 ± 697	22 646 ± 1778	6.05 ± 0.85
35	3	0.88 ± 0.75	2923 ± 393	20 885 ± 1837	4.56 ± 0.64
37	3	1.69 ± 0.59	1830 ± 365	16 124 ± 2931	5.14 ± 1.28
38	3	1.00 ± 0.71	2683 ± 471	22 428 ± 4994	5.70 ± 0.63
13	3	0.56 ± 0.31	1638 ± 326	5350 ± 709	3.55 ± 1.80
	1	1.75 ± 0.5	165 ± 31	943 ± 74	3.23 ± 0.65
41	3	1.19 ± 0.94	1494 ± 428	7005 ± 622	6.34 ± 2.79
	1	1.56 ± 0.88	257 ± 38	1016 ± 263	3.50 ± 0.73
42	3	0.75 ± 0.29	1398 ± 212	5352 ± 411	5.66 ± 1.24

^aData are presented as the mean ± SD from four male Sprague–Dawley rats.

(BF₃·Et₂O)⁴³ and triethylsilane (or Et₃SiD) with trifluoroacetic acid.^{44,45} After removing the methyl group on **17** or **18** with boron tribromide in methylene chloride, **19** or **20** was obtained in 75% yield.⁴⁶ The phenolic hydroxyl group of **19** or **20** was then protected with TBDMS-Cl using triethylamine as the base, yielding **21** or **22**.⁴⁷ Further lithium–halogen exchange of bromodiarylmethane **21** or **22** followed by the addition of the resulting aryllithium to 2,3,4,6-tetra-*O*-trimethylsilyl-β-D-glucosylactone and the subsequent etherification with methanol in the presence of hydrochloric acid provided desilylated *O*-methyl lactol **23** or **24**.^{48,49}

C-Aryl glycosides **11**, **25**, **26**, and **27** were synthesized according to Scheme 2. Stereoselective reduction of **23** and **24** using a combination of triethylsilane and boron trifluoride etherate (BF₃·Et₂O) in a mixture of methylene chloride and acetonitrile gave desired *C*-aryl glycosides **11** and **26** in 60–65% yield.^{50,51} Site-deuterated *C*-aryl glycosides **25** and **27** were prepared via a similar reduction of **23** and **24** with Et₃SiD (97% D).

Tosylated compounds **29–33** were prepared from *p*-toluenesulfonyl chloride **28** and appropriate alcohols (ROH, R = CH₂CH₃, CD₂CD₃, CD₂CH₃, CH₃, or CD₃), as shown in Scheme 3.⁵² The preparation of the target compounds **5**, **13**, and **34–43** was finally achieved according to Scheme 3. Coupling of

11 with **29–33** prepared above using cesium carbonate in DMF gave *C*-aryl glycosides **5**, **34–35**, **13**, and **41**.⁵³ Under similar conditions, coupling of **25–27** with TsOR using cesium carbonate in DMF gave deuterated *C*-aryl glycosides **36–40** and **42–43** in 68–75% yield.

RESULTS AND DISCUSSION

The in vitro inhibition activities of newly synthesized compounds on SGLT2 and SGLT1 were evaluated in cell-based SGLT functional assays in which inhibition of the rate of glucose uptake was monitored with CHO-K1 cells expressing human SGLT1 (*hSGLT1*) and SGLT2 (*hSGLT2*). For the SGLT2 assay, 293.ETN cells expressing *hSGLT2* were used, whereas COS-7 cells expressing *hSGLT1* were used to measure SGLT1 inhibition. Sodium-dependent glucopyranoside uptake was measured by subtracting the values obtained with a sodium-free buffer from those obtained using a sodium-containing buffer, and triplicate determinations were made for each test compound. The IC₅₀ values of the test compounds against SGLT2 and SGLT1 were determined, and the selectivity for SGLT2 inhibition was assessed. As shown in Table 1, when the hydrogens at the X, Y, or R sites were replaced partly or totally with deuteriums, the in vitro activities against SGLT2 of compounds **35**, **38**, **39**, **40**, and **43** showed about a 2-fold loss

Table 3. Pharmacokinetic Parameters after Oral and IV Administration to SD Rats^a

compound	route	PK in rat (1 mg/kg dose)					
		t_{\max} (h)	C_{\max} (ng/mL)	AUC _{0-∞} (ng h/mL)	$t_{1/2}$ (h)	CL (L/h/kg)	F%
41	p.o.	1.56 ± 0.88	257 ± 38	1016 ± 263	3.50 ± 0.73		76.3 ± 19.7
	i.v.			1332 ± 195	2.69 ± 0.32	0.76 ± 0.12	
13	p.o.	1.75 ± 0.5	165 ± 31	943 ± 74	3.23 ± 0.65		77.0 ± 6.0
	i.v.			1225 ± 226	2.09 ± 0.25	0.84 ± 0.17	

^aData are presented as the mean ± SD from four male Sprague–Dawley rats.

Table 4. Effects on Urinary Glucose Excretion in SD Rats^a

compound	urinary glucose excretion in SD rats (mg) (% relative to ref 5) (mean ± SD)		
	0–4 h	4–24 h	0–24 h
5	191 ± 48 (100%)	2231 ± 353 (100%)	2422 ± 361 (100%)
34	145 ± 67 (76%)	2151 ± 548 (96%)	2297 ± 548 (95%)
35	119 ± 73 (82%)	2311 ± 774 (98%)	2431 ± 789 (97%)
36	193 ± 24 (101%)	2457 ± 369 (110%)	2650 ± 385 (109%)
37	168 ± 17 (88%)	2057 ± 835 (92%)	2225 ± 842 (92%)
38	137 ± 9 (92%)	1941 ± 396 (91%)	2078 ± 391 (91%)
13	233 ± 35 (122%)	1657 ± 354 (74%)	1889 ± 361 (78%)
41	251 ± 44 (131%)	1983 ± 167 (89%)	2234 ± 199 (92%)
42	101 ± 38 (70%)	1994 ± 303 (84%)	2096 ± 332 (83%)
43	166 ± 24 (111%)	1483 ± 254 (69%)	1649 ± 242 (72%)
vehicle control	1.82 ± 3.78 (0.07%)	5.04 ± 0.69 (0.23%)	5.17 ± 0.72 (0.21%)

^aEach test compound was dissolved in 30% poly(ethylene glycol) (PEG400, average molecular weight of 400) and administered orally to overnight-fasted Sprague–Dawley rats ($n = 3$ per group) by gavage at the 1 mg/kg dose level. Control rats were given 30% PEG400 only. One hour postdosing, a glucose solution (2 g/kg, 10 mL/kg) was administered by oral gavage. Each value represents the mean ± SD.

Table 5. Effects on Urinary Glucose Excretion in Beagle dogs^a

compound	urinary glucose excretion in beagle dog (mg) (% relative to ref 5) (mean ± SD)		
	0–8 h	8–24 h	0–24 h
5	2155 ± 854 (100%)	9455 ± 2271 (100%)	11 610 ± 1677 (100%)
34	3472 ± 622 (161%)	8491 ± 1569 (90%)	11 964 ± 2190 (103%)
36	3765 ± 808 (175%)	8910 ± 1700 (94%)	12 676 ± 2150 (109%)
37	3396 ± 442 (158%)	6832 ± 2555 (72%)	10 228 ± 895 (88%)
38	4362 ± 818 (114%)	10 995 ± 1987 (95%)	15 357 ± 2514 (99%)
13	3620 ± 470 (168%)	10 876 ± 1303 (115%)	14 497 ± 1656 (125%)
41	3485 ± 596 (162%)	11 197 ± 3579 (118%)	14 682 ± 4172 (127%)
vehicle control	8.19 ± 3.04 (0.4%)	16.86 ± 4.59 (0.2%)	25.05 ± 6.81 (0.2%)

^aEach test compound was dissolved in 10% PEG400 and administered orally to overnight-fasted beagle dogs ($n = 3$ per group) by gavage at the 0.03 mg/kg dose level. Control dogs were given 10% PEG400 only. One hour postdosing, a glucose solution (2 g/kg, 5 mL/kg) was administered by oral gavage. Each value represents the mean ± SD.

of activity compared to parent compound 5, whereas other compounds exhibited the same or improved activity against SGLT2 compared to parent compound 5. With the exception of compounds 13 and 41–42, all other deuterated compounds showed the same or less potent activity against SGLT1 compared to compound 5. For example, compounds 34 and 36 exhibited slightly improved SGLT2 inhibitory activities compared to 5. With the exception of 38, all five derivatives (34, 37, 39, and 40) exhibited a slightly better selectivity than 5. Compounds 41–43 also exhibited a slightly better selectivity than the parent compound 13, indicating that deuterium substitution maintained SGLT2 inhibitory activity and improved the inhibitory selectivity for SGLT2 versus SGLT1.

The pharmacokinetic profiles of the deuterated analogues in male Sprague–Dawley (SD) rats were also assessed. As shown in Table 2, deuterated compounds 34–35, 37, and 38 generally displayed better PK properties as compared to parent compound 5 at the 3 mg/kg dose. In particular, compound 34 exhibited an

almost 2-fold increase in AUC_{0-∞} (ng h/mL) (22 646 ± 1778) compared to 5 (11 658 ± 2918). Its $t_{1/2}$ was also increased to 6.05 ± 0.85 h compared to that of 5 (4.52 ± 0.98 h). Similarly, deuterated compounds 41 and 42 also displayed slightly better PK properties than the parent compound 13. The $t_{1/2}$ of 41 and 42 (6.34 ± 2.79 and 5.66 ± 1.24 h, respectively) were found to be greater than that of 13 (3.55 ± 1.80 h) and were also greater than that of 5 (4.52 ± 0.98 h). Of note, 41 exhibited the longest $t_{1/2}$ among all the test compounds.

To compare the pharmacokinetics profiles of deuterated compound 41 and parent nondeuterated compound 13 further, we assessed these two compounds in male Sprague–Dawley (SD) rats ($n = 4$ per group) at a dose other than 3 mg/kg (i.e., 1 mg/kg). As shown in Table 2, the pharmacokinetics profiles of 41 and 13 in the rats orally dosed were poorer at the lower dose (i.e., 1 mg/kg) than at the higher dose (i.e., 3 mg/kg). Compounds 41 and 13 were administered both orally (p.o.) and intravenously (i.v.). As shown in Table 3, the key findings

from this experiment were that although **41** and **13** showed similar oral bioavailability ($F\%$) (76.3 ± 19.7 and 77.0 ± 6.0 , respectively), **41** showed a greater C_{\max} (ng/mL, p.o.) than **13** (257 ± 38 and 165 ± 31 , respectively). Moreover, **41** and **13** seemed to exhibit similar values for other PK parameters.

The effects of the deuterated analogues on urinary glucose excretion (UGE) in normal male Sprague–Dawley (SD) rats were also evaluated, and the results are reported as milligrams of glucose per 200 g of body weight in 24 h. As shown in Table 4, compound **36** exhibited a higher UGE than **5** for three different time periods, and **34**, **35**, **37**, and **38** exhibited similar UGE activities to that of **5**. Similarly, compound **41** was also observed to exhibit a higher UGE in the 4–24 and 0–24 h time periods than **13**. Compound **41** was also observed to exhibit a higher UGE in the 0–4 h period and a slightly lower UGE in the 0–24 h period than **5**. Compounds **42** and **43** exhibited similar or better UGE activities than **13** but slightly lower UGE activities than **5** in the 0–24 h period. It was found that the derivatives of **5** or **13** deuterated at only one metabolite site, such as **36** (deuterated at the A site) and **41** (deuterated at the C site), exhibited better UGE activities in SD rats.

Assessment of the UGE in dogs was also performed, and the results are summarized in Table 5. Compared with **5**, all test compounds except **38** (i.e., **34**, **36**, **37**, **13**, and **41**) induced 58–75% more UGE at the 0–8 h period. Consistent with the results in SD rats, compound **36** ($12\,676 \pm 2150$ mg) and **41** ($14\,682 \pm 4172$ mg) exhibited slightly more UGE than **5** ($11\,610 \pm 1677$ mg) during the 0–24 h period after compound administration. Among all of the tested deuterated analogues, **41** exhibited the most significant effect on UGE (0–24 h) in dogs.

We further performed the UGE and oral glucose-tolerance tests on compound **41** in normal male SD Rats. Compound **41** was found to lower blood glucose levels after a 2 g/kg glucose challenge. The baseline-corrected blood glucose AUC values observed following administration of 0.1, 0.3, 1, 3, and 10 mg/kg of **41** were 18.6, 20.7, 26.7, 21.6, and 5.0% that of the control AUC, respectively (Figure 7). These results indicated that **41** could significantly lower the blood glucose level in rats and could blunt the normal physiological response to a high dietary glucose load. Compound **41** was also found to increase the UGE significantly in a dose-dependent manner for all of the doses tested (Figure 8). It should be pointed out that although an

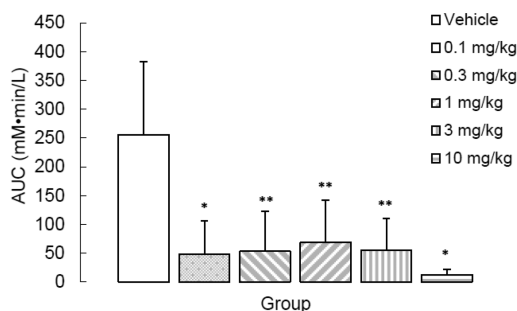


Figure 7. Effects of compound **41** on blood glucose levels in glucose-loaded Sprague–Dawley rats ($n = 5$ per group). Rats were fasted overnight and treated with a single oral dose of compound (0.1–10 mg/kg of **41**) 1 h prior to receiving the glucose challenge (20%, 2 g/kg, p.o.). Blood samples were obtained at –60, 0, 30, 60, 90, and 120 min. Blood glucose levels were then measured using a glucometer. Values of AUC (0–2 h) stand for baseline-corrected values calculated using the trapezoidal rule. Values represent the mean \pm SD. * $p < 0.01$ and ** $p < 0.05$ vs vehicle control.

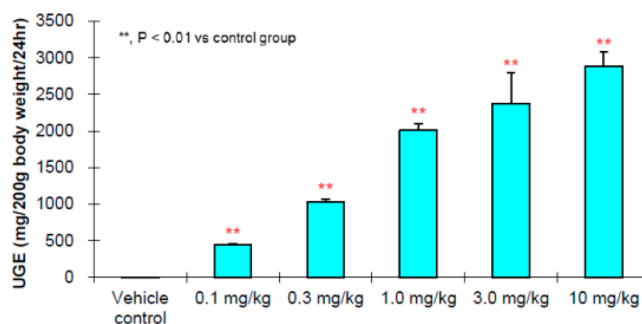


Figure 8. Rat 24 h UGE following treatment with **41**. Male Sprague–Dawley rats ($n = 5$ per group) were randomized to receive one of five doses of compound **41** (0.1, 0.3, 1, 3, and 10 mg/kg) by oral gavage. The test compound was dissolved in 30% PEG400. Control rats were given 30% PEG400 only. One hour postdosing, a glucose solution (2 g/kg, 10 mL/kg) was administered by oral gavage. Following compound administration, urine was collected over 24 h for measurement of UGE.

essentially linear dose–response curve was observed in Figure 8, a bell-curve was observed in Figure 7. In our opinion, these observations could be explained as follows: the initial **41**-induced withdrawal of glucose from the bloodstream would likely stimulate a compensatory response in a rat to produce/secrete more glucose into the bloodstream (from liver) in an attempt to maintain the blood glucose concentration, especially during a long (2 h) period of time; however, the dramatic increase in **41** (to 10 mg/kg) would overcome this natural compensatory response, leading to the observed dramatic decline in the blood glucose concentration. However, this would not have a linear correspondence to the UGE response because of the presence of another layer of the control (i.e., filtration in kidney). Therefore, a bell-curve was observed in Figure 7, and an essentially linear dose–response curve was still observed in Figure 8.

Comparative studies of the in vivo metabolism of deuterated compound **41** and nondeuterated compounds **13** and **5** were performed in rats. Compounds **41**, **13**, and **5** were dosed orally (50 mg/kg) to male Sprague–Dawley rats for five consecutive days, and all urine samples were collected and analyzed for metabolites. The HPLC-MS spectra and the proposed metabolites for **41** are shown in Figures 9, S1, and S2. Compound **11** was observed to be the major metabolite of **41** and **13**, but 87% of **41** remained unchanged, compared to 73% of **13** (0.84-fold that of **41**), indicating that deuterated compound **41** was more stable in vivo than **13**. We found that compound **5** not only had a de-ethylation metabolite (**11**, 41% by HPLC) but also had a hydroxylation metabolite (**12**, 16% by HPLC),³⁴ and unchanged **5** was observed during our HPLC analysis to constitute 43% of the parent plus metabolites (0.49-fold that of **41**). Compound **41** exhibited a low dealkylation (13%) compared to **5** (41%). Also, as shown in Figure 10, only one major metabolite was found for compound **41**, and the conversion rate of parent to metabolite (13%) in vivo for this compound was also the lowest compared to other compounds, which may lead to less concern over the formation of the methine-quinone metabolite from **41**.

CONCLUSIONS

We have designed and synthesized one class of potent, selective, and long-acting SGLT2 inhibitors through deuteration at the potential metabolic hotspots of known SGLT2 inhibitors. Among the deuterated compounds studied, compounds **34**, **36**, **41**, and **42** exhibited slightly stronger in vitro inhibitory activity

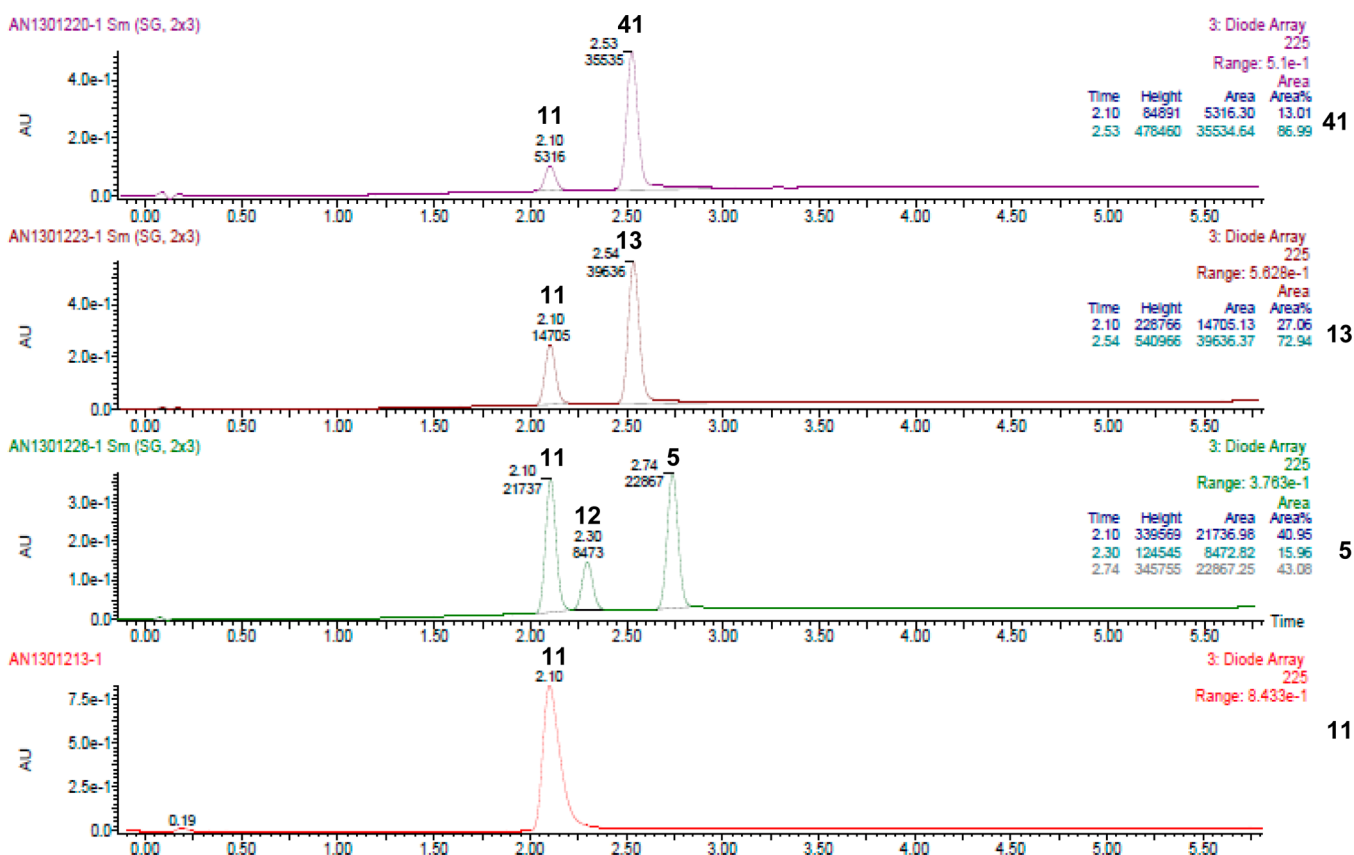


Figure 9. Overlay of the HPLC chromatograms showing the metabolites of **41**, **13**, **5**, and **11**. Compound **11** was used as a reference.

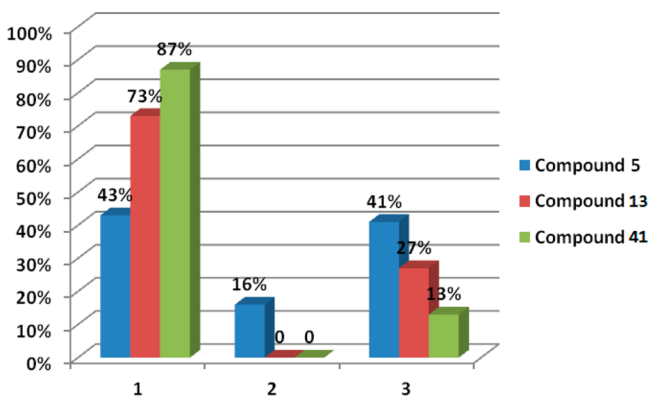


Figure 10. Conversion of parent compounds into metabolites. 1, 2, and 3 on *x* axis refer to the parent compound, the hydroxylation metabolite (**12**), and the dealkylation metabolite (**11**), respectively.

against *h*SGLT2 than nondeuterated compound **5**. The pharmacokinetics studies in SD rats revealed that the $t_{1/2}$ of **41** was increased the most among all of the deuterated analogues compared to the nondeuterated compounds (**5** and **13**). It was observed that deuteration at only one metabolic site, exemplified by **36** (deuterated at A site) and **41** (deuterated at C site), might be enough to improve UGE activities in SD rats. Compound **41** also exhibited an increase in UGE in beagle dogs versus **5** in the 0–24 h period. Compound **41** caused a dose-dependent increase in UGE in SD rats for all of the doses tested. Analysis of the in vivo metabolite profiles revealed that **41** had the least metabolites and was devoid of the hydroxylation metabolite (**12**), confirming the hypothesis that deuteration would reduce oxidative metabolism. In summary, via the C–D for C–H replacement

at the principal oxidative metabolic site, resulting deuterated compound **41** exhibited improved in vivo PK/ADME profiles, in vivo metabolite profiles, and in vivo efficacy in SD rats compared to nondeuterated compound **13**. As a potentially selective and long-acting SGLT2 inhibitor, compound **41** may warrant further assessment as an antidiabetic drug candidate.

EXPERIMENTAL SECTION

Chemistry. Unless specified otherwise, starting materials were generally available from commercial sources. Commercial grade anhydrous solvents were purchased from SK Chemical. Silica gel (Qingdao Haiyang) was used for analytical TLC (F254 plates) and flash chromatography (200–300 mesh). ^1H and ^{13}C NMR spectra were recorded on a Bruker 400 and 600 MHz instrument using CDCl_3 , CD_3OD , or acetone- d_6 as the solvent and TMS as the internal reference. Chemical shifts (δ) are expressed in parts per million (ppm) relative to the residual solvent peak (for chloroform-*d*, $\delta(^1\text{H}) = 7.26$ ppm and $\delta(^{13}\text{C}) = 77.16$ ppm; for methanol-*d*, $\delta(^1\text{H}) = 3.31$ ppm and $\delta(^{13}\text{C}) = 49.00$ ppm; and for acetone-*d*, $\delta(^1\text{H}) = 2.05$ ppm and $\delta(^{13}\text{C}) = 29.84$ ppm). Abbreviations used for signal patterns are as follows: s, singlet; d, doublet; dd, doublet of doublets; ddd, doublet of doublet of doublets; t, triplet; q, quadruplet; and m, multiplet. The high-pressure liquid chromatography–mass spectrometry (HPLC–MS) system employed a Waters ZQ2000 mass spectrometer interfaced with a Waters series 2695 liquid chromatograph and a Waters 2996 photodiode array detector. Electrospray ionization (ESI) was used as the ionization technique. MS analysis was performed in either positive or negative mode. Chromatographic separation was achieved using a Waters XTerra C18 column (3.5 μm , 50 \times 2.1 mm column). The column temperature was 35 $^\circ\text{C}$. The mobile phases A and B were 0.03% formic acid in acetonitrile and 0.05% formic acid in Milli-Q water, respectively. Gradient elution from 10 to 95% solvent A in 4.5 min at a flow rate of 0.8 mL/min and a final hold of 1.5 min at 95% A were employed. The total run time was 6 min. The photodiode array detector used wavelengths between 190 and 400 nm

(or 225 nm). The preparative HPLC-MS system employed a Waters ZQ2000 mass spectrometer interfaced with a Waters series 2525 liquid chromatograph and a Waters 2487 UV absorbance detector. The mobile phases A and B were 100% acetonitrile and 0.1% formic acid in Milli-Q water, respectively. Chromatographic separation was achieved using a Waters XTerra Prep MS C18 OBD column (5 μ m, 19 \times 100 mm column). A gradient elution was performed from 33 to 95% A in 15 min followed by a 5 min isocratic step at 95% A at a flow rate of 17 mL/min. UV absorbance at 225 nm was used to monitor the chromatography. High-resolution mass spectrometry (HRMS) was performed with an Agilent model 6210 time-of-flight instrument. Where the intensity of single chlorine ions is described, the expected intensity ratio was observed (approximately 3:1 for $^{35}\text{Cl}/^{37}\text{Cl}$ -containing ions), and the intensity of only the lower mass ion is given. GC was measured by a FULI 9790II gas chromatograph. The measurement conditions for GC were as follows: column, SE-54 (30 m \times 0.32 mm \times 0.25 μ m); detector, flame ionization (hydrogen gas flame); detector temperature, 280 $^{\circ}\text{C}$; split ratio, 10:1; inlet temperature, 250 $^{\circ}\text{C}$; flow (N_2), 3 mL/min; flow (H_2), 30 mL/min; flow (air), 300 mL/min; and column temperature program, column oven was started from 220 $^{\circ}\text{C}$, held for 2 min, and raised to 300 $^{\circ}\text{C}$ at a rate of 20 $^{\circ}\text{C}/\text{min}$ with a final hold of 10 min at 300 $^{\circ}\text{C}$. Analytical HPLC was measured by a 2690/2996 from Waters. The measurement conditions for HPLC were as follows: (condition I) column, Waters Sunfire C18 4.6 mm \times 250 mm, 5 μ m; mobile phases A and B, 0.05% formic acid in acetonitrile and 0.05% formic acid in Milli-Q water, respectively; gradient elution from 25 to 45% solvent A in 5 min followed by 45 to 90% solvent A in 15 min at a flow rate of 1.0 mL/min and a final hold of 10 min at 90% A; total run time, 30 min; and column temperature, 30 $^{\circ}\text{C}$. The photodiode array detector used a 225 nm wavelength. Condition II: column, Waters Sunfire C18 4.6 mm \times 250 mm, 5 μ m; mobile phases A and B, 0.05% formic acid in acetonitrile and 0.05% formic acid in Milli-Q water, respectively; gradient elution from 50 to 100% solvent A in 20 min at a flow rate of 1.0 mL/min and a hold of 19.5 min at 100% A followed by 50% A in 0.5 min; total run time, 40 min; column temperature, 30 $^{\circ}\text{C}$. The photodiode array detector used a 225 nm wavelength. All of the test compounds were determined to be >95% pure by HPLC.

(2S,3R,4R,5S,6R)-2-(4-Chloro-3-(4-ethoxybenzyl)phenyl)-6-(hydroxymethyl)tetrahydro-2H-pyran-3,4,5-triol (5). To a stirred solution of **11** (100 mg, 0.263 mmol) and **29** (57.9 mg, 0.289 mmol) in *N,N*-dimethylformamide (1.5 mL) was added cesium carbonate (257 mg, 0.789 mmol) followed by addition of tetrabutylammonium iodide (9.7 mg, 0.026 mmol). After stirring for 12 h at 40 $^{\circ}\text{C}$ under argon, the mixture was quenched by addition of ice water (10 mL). The mixture was extracted with ethyl acetate (2 \times 20 mL). The combined organic layers were washed with water (20 mL) and brine (20 mL), dried over anhydrous sodium sulfate, and concentrated, and the residue was purified by preparative TLC (thin-layer chromatography) to give product **5** (80.6 mg, 75% yield, HPLC purity (condition I): 99.8%) as a white solid. ^1H NMR (400 MHz, CD_3OD): δ 7.35–7.32 (m, 2H), 7.27 (dd, J = 2.0, 8.0 Hz, 1H), 7.09 (d, J = 8.8 Hz, 2H), 6.79 (d, J = 8.8 Hz, 2H), 4.10–4.01 (m, 3H), 3.98 (q, J = 7.2 Hz, 2H), 3.87 (d, J = 11.2 Hz, 1H), 3.69 (dd, J = 5.2, 12.0 Hz, 1H), 3.47–3.43 (m, 1H), 3.42–3.38 (m, 2H), 3.29–3.26 (m, 1H), 1.36 (t, J = 7.2 Hz, 3H). ^{13}C NMR (100 MHz, CD_3OD): δ 158.8, 140.0, 139.9, 134.4, 132.8, 131.9, 130.8, 130.1, 128.2, 115.4, 82.9, 82.2, 79.7, 76.4, 71.8, 64.4, 63.0, 39.2, 15.2. MS (ESI) m/z 431 ($\text{M} + \text{Na}^+$, positive mode), 453 ($\text{M} + \text{HCO}_2^-$, negative mode). HRMS: m/z calcd for $\text{C}_{21}\text{H}_{25}\text{ClNaO}_6$ ($\text{M} + \text{Na}^+$), 431.1232; found, 431.1232.

(2S,3R,4R,5S,6R)-2-(4-Chloro-3-(4-hydroxybenzyl)phenyl)-6-(hydroxymethyl)tetrahydro-2H-pyran-3,4,5-triol (11). To a solution of **23** (1.03 g, 2.50 mmol) in dichloromethane (10.0 mL) and acetonitrile (10.0 mL) at -30 $^{\circ}\text{C}$ under argon was added triethylsilane (1.6 mL, 10.0 mmol, 97 atom % D). Then, boron trifluoride etherate (0.95 mL, 7.50 mmol) was added while maintaining the reaction temperature below -15 $^{\circ}\text{C}$, and the reaction mixture was stirred for another 2 h at -20 to -10 $^{\circ}\text{C}$. The reaction was quenched by addition of 5% sodium bicarbonate until reaching pH 7.5. The organic phase was separated, and the aqueous phase was extracted with ethyl acetate (3 \times 30 mL). The combined organic phases were washed with brine (2 \times 50

mL) and dried over anhydrous sodium sulfate. The sample was concentrated under reduced pressure to provide a pale solid product, which was purified by the flash chromatography to give product **11** (571 mg, 60% yield, HPLC purity (condition I): 99.0%) as a white solid. ^1H NMR (400 MHz, CD_3OD): δ 7.34 (d, J = 8.0 Hz, 1H), 7.31 (d, J = 1.6 Hz, 1H), 7.26 (dd, J = 2.0, 8.0 Hz, 1H), 7.01 (d, J = 8.4 Hz, 2H), 6.68 (d, J = 8.4 Hz, 2H), 4.08 (d, J = 9.6 Hz, 1H), 4.02 (d, J = 15.2 Hz, 1H), 3.96 (d, J = 15.2 Hz, 1H), 3.87 (d, J = 11.6 Hz, 1H), 3.69 (dd, J = 5.6, 11.6 Hz, 1H), 3.47–3.44 (m, 1H), 3.42–3.38 (m, 2H), 3.30–3.27 (m, 1H). ^{13}C NMR (100 MHz, CD_3OD): δ 156.7, 140.1, 139.9, 134.4, 131.9, 131.7, 130.8, 130.1, 128.1, 116.1, 82.9, 82.2, 79.7, 76.4, 71.8, 63.1, 39.2. MS (ESI) m/z 403 ($\text{M} + \text{Na}^+$, positive mode), 425 ($\text{M} + \text{HCO}_2^-$, negative mode).

(2S,3R,4R,5S,6R)-2-(4-Chloro-3-(4-methoxybenzyl)phenyl)-6-(hydroxymethyl)tetrahydro-2H-pyran-3,4,5-triol (13). Compound **13** (72.7 mg, 70% yield, HPLC purity (condition I): 99.9%) was prepared as a white solid from **11** (100 mg, 0.263 mmol) and **32** (53.8 mg, 0.289 mmol) according to the method described for the synthesis of **5**. ^1H NMR (400 MHz, CD_3OD): δ 7.34 (d, J = 8.4 Hz, 1H), 7.32 (d, J = 2.0 Hz, 1H), 7.27 (dd, J = 2.0, 8.4 Hz, 1H), 7.10 (d, J = 8.8 Hz, 2H), 6.81 (d, J = 8.8 Hz, 2H), 4.07–3.98 (m, 3H), 3.87 (d, J = 11.6 Hz, 1H), 3.75 (s, 3H), 3.69 (dd, J = 5.2, 12.0 Hz, 1H), 3.46–3.42 (m, 1H), 3.41–3.35 (m, 2H), 3.30–3.27 (m, 1H). ^{13}C NMR (100 MHz, CD_3OD): δ 159.6, 140.0, 139.9, 134.4, 133.0, 131.9, 130.8, 130.1, 128.2, 114.8, 82.9, 82.2, 79.7, 76.4, 71.9, 63.1, 55.6, 39.2. MS (ESI) m/z 412 ($\text{M} + \text{NH}_4^+$, positive mode), 439 ($\text{M} + \text{HCO}_2^-$, negative mode). HRMS: m/z calcd for $\text{C}_{20}\text{H}_{23}\text{ClNaO}_6$ ($\text{M} + \text{Na}^+$), 417.1075; found, 417.1079.

5-Bromo-2-chlorobenzoyl chloride (15). *N,N*-Dimethylformamide (0.1 mL) was added to a suspension of 5-bromo-2-chlorobenzoic acid (23.6 g, 100 mmol) and oxalyl chloride (15.2 g, 120 mmol) in a 500 mL four-necked flask containing dichloromethane (118 mL) at room temperature. Once the vigorous evolution of gas ceased, the reaction was stirred for 10 h at room temperature. The reaction mixture was concentrated under vacuum to give product **15** (25.4 g, 100%) as an off-white solid. ^1H NMR (400 MHz, CDCl_3): δ 8.19 (d, J = 2.4 Hz, 1H), 7.64 (dd, J = 2.4, 8.8 Hz, 1H), 7.38 (d, J = 8.8 Hz, 1H). ^{13}C NMR (100 MHz, CDCl_3): δ 164.1, 137.4, 135.8, 134.5, 132.9, 132.7, 120.6.

(5-Bromo-2-chlorophenyl)(4-methoxyphenyl)methanone (16). A 250 mL four-necked flask equipped with an internal thermometer was charged with anisole (5.68 g, 52.5 mmol) and dichloromethane (19 mL) under argon. The mixture was stirred for 10 min at room temperature and cooled to -5 to 0 $^{\circ}\text{C}$. Aluminum(III) chloride (7.33 g, 55 mmol) was added portionwise to the above solution over 30 min while maintaining the internal temperature below 0 $^{\circ}\text{C}$. After the addition was complete, the reaction mixture was stirred for another 30 min at -5 to 0 $^{\circ}\text{C}$, and a solution of 5-bromo-2-chlorobenzoyl chloride (12.7 g, 50 mmol) in dichloromethane (19 mL) was added via an addition funnel over 30 min while keeping the reaction temperature below 0 $^{\circ}\text{C}$. After the addition was completed, the reaction mixture was stirred for another 1.5 h at -5 to 0 $^{\circ}\text{C}$ under argon. The reaction was poured into ice water (150 g) with stirring, and dichloromethane (100 mL) and concentrated hydrochloric acid (5 mL) were added. The organic layer was separated, and the aqueous layer was extracted with dichloromethane (100 mL). The combined organic layers were washed with water (100 mL), saturated aqueous sodium bicarbonate (100 mL), and brine (100 mL), dried over sodium sulfate (10 g), and concentrated. The residue was recrystallized in absolute ethanol (75 mL) to give title compound **16** as a white solid (13.5 g, 83% yield, HPLC purity (condition II): 99.9%, GC purity: 99.7%). ^1H NMR (400 MHz, CDCl_3): δ 7.78 (d, J = 8.8 Hz, 2H), 7.53 (dd, J = 2.0, 8.4 Hz, 1H), 7.48 (d, J = 2.4 Hz, 1H), 7.32 (d, J = 8.8 Hz, 1H), 6.95 (d, J = 8.8 Hz, 2H), 3.89 (s, 3H). ^{13}C NMR (100 MHz, CDCl_3): δ 192.2, 164.5, 140.8, 133.9, 132.7, 131.7, 131.6, 130.2, 128.9, 120.6, 114.2, 55.7. MS (ESI) m/z 325 ($\text{M} + \text{H}^+$, positive mode).

4-Bromo-1-chloro-2-(4-methoxybenzyl)benzene (17). To a stirred solution of (5-bromo-2-chlorophenyl)(4-methoxyphenyl)methanone (**16**) (6.51 g, 20 mmol) and sodium borohydride (757 mg, 20 mmol) in tetrahydrofuran (52 mL) was slowly added aluminum chloride (2.67 g, 20 mmol) over 1 h at 5 to 10 $^{\circ}\text{C}$ under argon. The reaction was warmed slowly to reflux for 5 h and cooled to 15 to 20 $^{\circ}\text{C}$.

Additional sodium borohydride (757 mg, 20 mmol) was added slowly over 1 h, and the reaction was refluxed for another 12 h. The reaction mixture was cooled to 15 to 20 °C, poured into ice water (100 mL), and then extracted with ethyl acetate (2 × 80 mL). The combined organic layers were washed with water (2 × 50 mL) and brine (50 mL) and concentrated under vacuum to give an off-white solid. This solid was dissolved in ethanol at 75 to 80 °C with stirring (6 mL), cooled to 0 to 5 °C, and stirred for 10 h. The mixture was filtered, and the filter cake was washed with precooled (−5 °C) ethanol (2 mL) and dried under vacuum to give product **17** (5.11 g, 82% yield, HPLC purity (condition I): 99.1%). ¹H NMR (400 MHz, CDCl₃): δ 7.26 (dd, *J* = 2.4, 8.4 Hz, 1H), 7.24–7.20 (m, 2H), 7.09 (d, *J* = 8.8 Hz, 2H), 6.84 (d, *J* = 8.8 Hz, 2H), 3.98 (s, 2H), 3.79 (s, 3H). ¹³C NMR (100 MHz, CDCl₃): δ 158.4, 141.4, 133.7, 133.2, 131.0, 130.7, 130.1, 120.6, 114.2, 55.4, 38.3.

4-Bromo-1-chloro-2-((4-methoxyphenyl)methyl-d₂)benzene (18).⁴² To a stirred solution of (5-bromo-2-chlorophenyl)(4-methoxyphenyl)methanone (**16**) (6.51 g, 20 mmol) and sodium borodeuteride (837 mg, 20 mmol) in tetrahydrofuran (52 mL) was slowly added aluminum chloride (2.67 g, 20 mmol) over 1 h at 5 to 10 °C under argon. The reaction was warmed slowly to reflux for 5 h and then cooled to 15 to 20 °C. Additional sodium borodeuteride (837 mg, 20 mmol) was added slowly over 1 h, and the reaction was refluxed for another 12 h. The reaction mixture was cooled to 15 to 20 °C, poured into ice water (100 mL), and then extracted with ethyl acetate (2 × 80 mL). The combined organic layers were washed with water (2 × 50 mL) and brine (50 mL) and concentrated under vacuum to give an off-white solid. The solid was dissolved in ethanol at 75 to 80 °C with stirring (6 mL), the mixture was cooled to 0 to 5 °C and stirred for 10 h. The mixture was filtered, and the filter cake was washed with precooled (−5 °C) ethanol (2 mL) and dried under vacuum to give product **18** (5.17 g, 83% yield, HPLC purity (condition II): 99.5%) as a white solid. ¹H NMR (400 MHz, CDCl₃): δ 7.27–7.24 (m, 2H), 7.21 (d, *J* = 8.0 Hz, 1H), 7.09 (d, *J* = 8.4 Hz, 2H), 6.84 (d, *J* = 8.4 Hz, 2H), 3.78 (s, 3H). ¹³C NMR (100 MHz, CDCl₃): δ 158.4, 141.3, 133.6, 133.2, 131.0, 130.7, 130.6, 130.1, 120.6, 114.2, 55.4.

4-(5-Bromo-2-chlorobenzyl)phenol (19). To a solution of **17** (4.67 g, 15 mmol) in dichloromethane (46.7 mL) at −20 °C was added boron tribromide (1.62 mL, 0.022 mol) over 10 min at a rate that maintained the reaction temperature below −10 °C under argon. After addition, the mixture was slowly warmed to 0 °C and stirred for 2 h. The reaction mixture was poured into 100 mL of ice water and extracted with dichloromethane (2 × 100 mL). The combined organic layers were washed with saturated bicarbonate (80 mL), water (80 mL), and brine (80 mL) and then dried over sodium sulfate. The sample was concentrated and purified by silica gel column chromatography to give product **19** (3.35 g, 75% yield, HPLC purity (condition II): 99.7%) as a white solid. ¹H NMR (400 MHz, CD₃OD): δ 7.33 (dd, *J* = 2.4, 8.4 Hz, 1H), 7.29–7.27 (m, 2H), 6.99 (d, *J* = 8.4 Hz, 2H), 6.72 (d, *J* = 8.4 Hz, 2H), 3.95 (s, 2H). ¹³C NMR (100 MHz, CD₃OD): δ 157.1, 143.2, 134.7, 134.2, 132.0, 131.7, 131.0, 130.8, 121.5, 116.4, 38.9. MS (ESI) *m/z* 295 (M − H⁺, negative mode), 341 (M + HCO₂[−], negative mode).

4-((5-Bromo-2-chlorophenyl)methyl-d₂)phenol (20).⁴⁶ To a solution of **18** (4.70 g, 15 mmol) in dichloromethane (46.7 mL) under argon at −20 °C was added boron tribromide (1.62 mL, 0.022 mol) over 10 min at a rate that maintained the reaction temperature below −10 °C. After addition, the mixture was slowly warmed to 0 °C and stirred for 2 h. The reaction mixture was poured into 100 mL of ice water and extracted with dichloromethane (2 × 100 mL). The combined organic layers were washed with saturated bicarbonate (80 mL), water (80 mL), and brine (80 mL) and then dried over anhydrous sodium sulfate. The sample was concentrated and purified by silica gel column chromatography to give product **20** (3.51 g, 78% yield, HPLC purity (condition II): 99.8%) as a white solid. ¹H NMR (400 MHz, CD₃OD): δ 7.31 (dd, *J* = 2.4, 8.4 Hz, 1H), 7.29 (d, *J* = 2.4 Hz, 1H), 7.26 (d, *J* = 8.0 Hz, 1H), 6.99 (d, *J* = 8.4 Hz, 2H), 6.72 (d, *J* = 8.4 Hz, 2H). ¹³C NMR (100 MHz, CD₃OD): δ 157.1, 143.1, 134.7, 134.1, 132.0, 131.7, 130.9, 130.6, 121.5, 116.4. MS (ESI) *m/z* 297 (M − H⁺, negative mode), 343 (M + HCO₂[−], negative mode).

4-(5-Bromo-2-chlorobenzyl)phenoxy(tert-butyl)dimethylsilane (21). To a stirred suspension of **19** (3.0 g, 10.1 mmol)

and *tert*-butylchlorodimethylsilane (1.82 g, 12.1 mol) in acetonitrile (30 mL) was added dropwise triethylamine (2.11 mL, 15.1 mmol) so that the reaction temperature did not exceed 5 °C. After the addition was completed, the reaction mixture was stirred for 2 h at 10 to 15 °C. This reaction mixture was filtered, and the filter cake was washed with petroleum ether (2 × 20 mL). The combined organic layers were evaporated under reduced pressure (30 °C), and the residue was dissolved in petroleum ether (30 mL). The solution was washed with water (2 × 30 mL) and evaporated, and the residue was dissolved in ethanol (9 mL) at 35 °C with stirring. This solution was cooled to 5 to 10 °C and kept for 4 h. The solids were filtered, and the filter cake was washed with precooled ethanol (0–5 °C, 3 mL) and then dried under vacuum at 20 to 25 °C for 16 h to give **21** (3.58 g, 86% yield, HPLC purity (condition II): 99.8%) as a white solid. ¹H NMR (400 MHz, CDCl₃): δ 7.27 (dd, *J* = 2.4, 8.4 Hz, 1H), 7.23–7.21 (m, 2H), 7.03 (d, *J* = 8.4 Hz, 2H), 6.78 (d, *J* = 8.4 Hz, 2H), 3.97 (s, 2H), 0.98 (s, 9H), 0.19 (s, 6H). ¹³C NMR (100 MHz, CDCl₃): δ 154.4, 141.5, 133.7, 133.2, 131.3, 131.0, 130.6, 130.1, 120.6, 120.3, 38.4, 25.8, 18.3, −4.3.

4-((5-Bromo-2-chlorophenyl)methyl-d₂)phenoxy(tert-butyl)dimethylsilane (22).⁴⁷ To a stirred suspension of **20** (3.0 g, 10 mmol) and *tert*-butylchlorodimethylsilane (1.80 g, 12.0 mol) in acetonitrile (30 mL) was added dropwise triethylamine (2.10 mL, 15.0 mmol) so that the reaction temperature did not exceed 5 °C. After the addition was completed, the reaction mixture was stirred for 2 h at 10 to 15 °C. This reaction mixture was filtered, and the filter cake was washed with petroleum ether (2 × 20 mL). The combined organic layers were evaporated under reduced pressure (30 °C), and the residue was dissolved in petroleum ether (30 mL). The solution was washed with water (2 × 30 mL) and evaporated, and the residue was dissolved in ethanol (9 mL) at 35 °C with stirring. The solution was cooled to 5 to 10 °C and kept for 4 h. The solids were filtered, and the filter cake was washed with precooled ethanol (0–5 °C, 3 mL) and then dried under vacuum at 20 to 25 °C for 16 h to give **22** (3.72 g, 90% yield, HPLC purity (condition II): 99.6%) as a white solid. ¹H NMR (400 MHz, CDCl₃): δ 7.28–7.20 (m, 3H), 7.03 (d, *J* = 8.4 Hz, 2H), 6.78 (d, *J* = 8.8 Hz, 2H), 0.98 (s, 9H), 0.19 (s, 6H). ¹³C NMR (100 MHz, CDCl₃): δ 154.4, 141.4, 133.7, 133.2, 131.2, 131.0, 130.7, 130.1, 120.6, 120.3, 25.8, 18.3, −4.3.

(2S,3R,4S,5S,6R)-2-(4-Chloro-3-(4-hydroxybenzyl)phenyl)-6-(hydroxymethyl)-2-methoxytetrahydro-2H-pyran-3,4,5-triol (23). To a solution of **21** (2.5 g, 6.1 mmol) in anhydrous toluene/tetrahydrofuran (15 mL, 2:1) at −65 °C was added dropwise *n*-BuLi (2.5 M in hexane, 2.92 mL), and the reaction was stirred for an additional 30 min at −65 °C under argon. A precooled (−30 °C) solution of (3R,4S,5R,6R)-3,4,5-tris(trimethylsilyloxy)-6-((trimethylsilyloxy)methyl)tetrahydro-2H-pyran-2-one (3.7 g, 7.9 mmol) in toluene (10 mL) was added slowly dropwise to the above reaction mixture and kept such that the reaction temperature did not exceed −60 °C. The mixture was stirred at −65 to −55 °C for 3 h. The reaction was quenched with hydrochloric acid (0.76 mL, 9.1 mmol) in methanol (10 mL), and the mixture was allowed to warm to 20 to 25 °C and stirred for 16 h. The reaction mixture was quenched by the addition of 5% aqueous sodium bicarbonate until the pH reached 7.5, and the organic phase was separated. The aqueous phase was extracted with ethyl acetate (2 × 30 mL), and the combined organic phases were washed with saturated bicarbonate (50 mL), water (50 mL), and brine (50 mL) and dried over sodium sulfate. After removal of the volatiles, the residue was dried under vacuum to give product **23** (2.0 g; 80%), which was used in the next step without further purification. ¹H NMR (400 MHz, CD₃OD): δ 7.53 (d, *J* = 2.0 Hz, 1H), 7.45 (dd, *J* = 2.0, 8.4 Hz, 1H), 7.35 (d, *J* = 8.4 Hz, 1H), 7.01 (d, *J* = 8.4 Hz, 2H), 6.68 (d, *J* = 8.8 Hz, 2H), 4.06 (d, *J* = 15.2 Hz, 1H), 3.98–3.91 (m, 2H), 3.81 (dd, *J* = 5.2, 12.0 Hz, 1H), 3.75 (t, *J* = 9.2 Hz, 1H), 3.58 (ddd, *J* = 2.0, 5.2, 7.6 Hz, 1H), 3.42 (t, *J* = 9.2 Hz, 1H), 3.09 (d, *J* = 9.2 Hz, 1H), 3.07 (s, 3H). ¹³C NMR (100 MHz, CD₃OD): δ 156.7, 139.8, 139.1, 134.9, 131.9, 130.8, 129.9, 128.2, 116.1, 102.4, 78.6, 76.0, 75.1, 71.7, 62.8, 39.3. MS (ESI) *m/z* 433 (M + Na⁺, positive mode), 455 (M + HCO₂[−], negative mode).

(3R,4S,5S,6R)-2-(4-Chloro-3-((4-hydroxyphenyl)methyl-d₂)phenyl)-6-(hydroxymethyl)-2-methoxytetrahydro-2H-pyran-3,4,5-triol (24).^{48,49} To a solution of **22** (2.48 g, 6.0 mmol) in

anhydrous toluene/tetrahydrofuran (15 mL, 2:1) at -65°C was added dropwise *n*-BuLi (2.5 M in hexane, 2.90 mL), and the reaction was stirred for an additional 30 min at -65°C under argon. A precooled (-30°C) solution of (3*R*,4*S*,5*R*,6*R*)-3,4,5-tris(trimethylsilyloxy)-6-((trimethylsilyloxy)methyl)tetrahydro-2*H*-pyran-2-one (3.64 g, 7.8 mmol) in toluene (10 mL) was added dropwise slowly to the above reaction mixture, and the reaction temperature was not allowed to exceed -60°C . The mixture was stirred at -65 to -55°C for 3 h. The reaction was quenched with hydrochloric acid (0.75 mL, 9.0 mmol) in methanol (10 mL), and the mixture was allowed to warm to 20 to 25°C and stirred for 16 h. The reaction mixture was quenched by the addition of 5% aqueous sodium bicarbonate until the pH reached 7.5, and the organic phase was separated. The aqueous phase was extracted with ethyl acetate (2 \times 30 mL), and the combined organic phases were washed with saturated bicarbonate (50 mL), water (50 mL), and brine (50 mL) and dried over sodium sulfate. After removal of the volatiles, the residue was dried under vacuum to give product **24** (1.86 g, 75%), which was used in the next step without further purification. ^1H NMR (400 MHz, CD_3OD): δ 7.53 (d, $J = 2.0$ Hz, 1H), 7.45 (dd, $J = 2.0, 8.4$ Hz, 1H), 7.35 (d, $J = 8.4$ Hz, 1H), 7.01 (d, $J = 8.4$ Hz, 2H), 6.68 (d, $J = 8.4$ Hz, 2H), 3.93 (dd, $J = 2.0, 12.0$ Hz, 1H), 3.81 (dd, $J = 5.6, 12.0$ Hz, 1H), 3.75 (t, $J = 9.2$ Hz, 1H), 3.61 (ddd, $J = 2.0, 5.2, 7.6$ Hz, 1H), 3.42 (t, $J = 9.6$ Hz, 1H), 3.09 (d, $J = 9.6$ Hz, 1H), 3.07 (s, 3H). ^{13}C NMR (100 MHz, CD_3OD): δ 156.7, 139.8, 139.1, 134.9, 131.8, 130.8, 129.9, 128.2, 116.1, 102.5, 78.6, 76.0, 75.1, 71.7, 62.8. MS (ESI) m/z 435 ($\text{M} + \text{Na}^+$, positive mode), 457 ($\text{M} + \text{HCO}_2^-$, negative mode). HRMS: m/z calcd for $\text{C}_{20}\text{H}_{21}\text{D}_2\text{ClO}_7$ ($\text{M} - \text{H}^+$), 411.1258; found, 411.1191.

(2*S*,3*R*,4*R*,5*S*,6*R*)-2-(4-Chloro-3-(4-hydroxybenzyl)phenyl)-2-*d*-6-(hydroxymethyl)tetrahydro-2*H*-pyran-3,4,5-triol (25**).** To a solution of **23** (205.4 mg, 0.50 mmol) in dichloromethane (2.0 mL) and acetonitrile (2.0 mL) at -30°C under argon was added triethylsilane-*d* (0.32 mL, 2.0 mmol, 97 atom % D). Then, boron trifluoride etherate (0.19 mL, 1.5 mmol) was added while maintaining the reaction temperature below -15°C , and the reaction mixture was stirred for another 2 h at -20 to -10°C . The reaction was quenched by addition of 5% sodium bicarbonate until reaching pH 7.5. The organic phase was separated, and the aqueous phase was extracted with ethyl acetate (3 \times 20 mL). The combined organic phases were washed with brine (2 \times 30 mL) and dried over anhydrous sodium sulfate. The sample was concentrated under reduced pressure to provide a pale solid product, which was purified by preparative HPLC to give product **25** as a white solid (125 mg, 65% yield, HPLC purity (condition I): 99.6%). ^1H NMR (400 MHz, CD_3OD): δ 7.34 (d, $J = 8.0$ Hz, 1H), 7.31 (d, $J = 1.6$ Hz, 1H), 7.26 (dd, $J = 2.0, 8.4$ Hz, 1H), 7.01 (d, $J = 8.4$ Hz, 2H), 6.68 (d, $J = 8.4$ Hz, 2H), 4.02 (d, $J = 15.2$ Hz, 1H), 3.96 (d, $J = 15.2$ Hz, 1H), 3.87 (d, $J = 12.0$ Hz, 1H), 3.68 (dd, $J = 5.2, 12.0$ Hz, 1H), 3.47–3.43 (m, 1H), 3.42–3.38 (m, 2H), 3.30–3.28 (m, 1H). ^{13}C NMR (100 MHz, CD_3OD): δ 156.8, 140.1, 139.9, 134.4, 131.9, 131.7, 130.9, 130.1, 128.1, 116.1, 82.2, 79.7, 76.4, 71.9, 63.1, 39.2. MS (ESI) m/z 382 ($\text{M} + \text{H}^+$, positive mode), 426 ($\text{M} + \text{HCO}_2^-$, negative mode).

(2*S*,3*R*,4*R*,5*S*,6*R*)-2-(4-Chloro-3-((4-hydroxyphenyl)methyl-*d*₂)phenyl)-6-(hydroxymethyl)tetrahydro-2*H*-pyran-3,4,5-triol (26**).** Compound **26** (474 mg, 62% yield, HPLC purity (condition I): 99.0%) was prepared as a white solid from **24** (826 mg, 2.0 mmol) according to the method described for the synthesis of **11**. ^1H NMR (400 MHz, CD_3OD): δ 7.34 (d, $J = 8.4$ Hz, 1H), 7.31 (d, $J = 2.0$ Hz, 1H), 7.26 (dd, $J = 2.0, 8.0$ Hz, 1H), 7.01 (d, $J = 8.4$ Hz, 2H), 6.68 (d, $J = 8.4$ Hz, 2H), 4.08 (d, $J = 9.2$ Hz, 1H), 3.87 (d, $J = 11.2$ Hz, 1H), 3.68 (dd, $J = 5.2, 12.0$ Hz, 1H), 3.47–3.43 (m, 1H), 3.43–3.38 (m, 2H), 3.30–3.27 (m, 1H). ^{13}C NMR (150 MHz, CD_3OD): δ 156.8, 140.1, 140.0, 134.4, 131.9, 131.7, 130.8, 130.1, 128.1, 116.2, 82.9, 82.2, 79.8, 76.5, 71.9, 63.1. MS (ESI) m/z 400 ($\text{M} + \text{NH}_4^+$, positive mode), 427 ($\text{M} + \text{HCO}_2^-$, negative mode).

(2*S*,3*R*,4*R*,5*S*,6*R*)-2-(4-Chloro-3-((4-hydroxyphenyl)methyl-*d*₂)phenyl)-2-*d*-6-(hydroxymethyl)tetrahydro-2*H*-pyran-3,4,5-triol (27**).**^{51,52} Compound **27** (461 mg, 60% yield, HPLC purity (condition I): 99.4%) was prepared as a white solid from **24** (826 mg, 2.0 mmol) according to the method described for the synthesis of **25**. ^1H NMR (400 MHz, CD_3OD): δ 7.34 (d, $J = 8.4$ Hz, 1H), 7.31 (d, $J = 2.0$ Hz, 1H), 7.26 (dd, $J = 2.0, 8.4$ Hz, 1H), 7.01 (d, $J = 8.4$ Hz, 2H), 6.68 (d,

$J = 8.4$ Hz, 2H), 3.87 (d, $J = 11.2$ Hz, 1H), 3.68 (dd, $J = 5.2, 12.0$ Hz, 1H), 3.47–3.43 (m, 1H), 3.42–3.36 (m, 2H), 3.29–3.26 (m, 1H). ^{13}C NMR (100 MHz, CD_3OD): δ 156.8, 140.1, 139.9, 134.4, 131.9, 131.7, 130.8, 130.1, 128.1, 116.1, 82.2, 79.7, 76.4, 71.9, 63.1. MS (ESI) m/z 401 ($\text{M} + \text{NH}_4^+$, positive mode), 428 ($\text{M} + \text{HCO}_2^-$, negative mode). HRMS: m/z calcd for $\text{C}_{19}\text{H}_{18}\text{D}_3\text{ClO}_6$ ($\text{M} - \text{H}^+$), 382.1215; found, 382.1140.

Ethyl 4-Methylbenzenesulfonate (29**).** To a stirred solution of ethanol (2.30 g, 50 mmol) in THF (11.5 mL) was added precooled (0– 5°C) aqueous sodium hydroxide (6 g NaOH in 32.6 mL of water). After stirring for 15 min and cooling to -5°C , *p*-toluenesulfonyl chloride **28** (10.5 g, 55 mmol) was added portionwise while keeping the reaction temperature so that it did not exceed 0°C . After the addition was completed, the reaction mixture was allowed to warm to 15 to 20°C and stirred for another 10 h. The reaction mixture was quenched by addition of ice water (100 mL). The mixture was extracted with dichloromethane (2 \times 80 mL), the combined organic layers were washed with saturated aqueous ammonium chloride (100 mL), water (100 mL), and brine (100 mL), dried over anhydrous sodium sulfate, and concentrated, and the residue was purified by flash silica gel column to give product **29** (6.61 g, 66%) as a white solid. ^1H NMR (400 MHz, CD_3COCD_3): δ 7.80 (d, $J = 8.4$ Hz, 2H), 7.48 (d, $J = 8.4$ Hz, 2H), 4.10 (q, $J = 7.2$ Hz, 2H), 2.46 (s, 3H), 1.24 (t, $J = 7.2$ Hz, 3H). ^{13}C NMR (100 MHz, CD_3COCD_3): δ 145.7, 134.6, 130.8, 128.6, 67.8, 21.5, 14.9. MS (ESI) m/z 201 ($\text{M} + \text{H}^+$, positive mode).

Ethyl-*d*₅ 4-Methylbenzenesulfonate (30**).** Compound **30** (6.68 g, 65%) was prepared as a white solid from ethanol-*d*₆ (2.61 g, 50 mmol, 99.5 atom % D) according to the method described for the synthesis of **29**. ^1H NMR (400 MHz, CD_3COCD_3): δ 7.80 (d, $J = 8.4$ Hz, 2H), 7.48 (d, $J = 8.4$ Hz, 2H), 2.45 (s, 3H). ^{13}C NMR (100 MHz, CD_3COCD_3): δ 145.7, 134.5, 130.8, 128.6, 21.5. MS (ESI) m/z 206 ($\text{M} + \text{H}^+$, positive mode).

Ethyl-1,1-*d*₂ Alcohol 4-Methylbenzenesulfonate (31**).** Compound **31** (3.44 g, 68%) was prepared as a white solid from ethyl-1,1-*d*₂ alcohol (1.20 g, 25 mmol, 98 atom % D) according to the method described for the synthesis of **29**. ^1H NMR (400 MHz, CD_3COCD_3): δ 7.80 (d, $J = 8.4$ Hz, 2H), 7.48 (d, $J = 8.0$ Hz, 2H), 2.46 (s, 3H), 1.23 (s, 3H). ^{13}C NMR (100 MHz, CD_3COCD_3): δ 145.7, 134.6, 130.8, 128.6, 21.5, 14.7. MS (ESI) m/z 203 ($\text{M} + \text{H}^+$, positive mode).

Methyl 4-Methylbenzenesulfonate (32**).** Compound **32** (12.7 g, 68%) was prepared as a white solid from methanol (3.2 g, 100 mmol) according to the method described for the synthesis of **29**. ^1H NMR (400 MHz, CD_3COCD_3): δ 7.80 (d, $J = 8.4$ Hz, 2H), 7.50 (d, $J = 8.4$ Hz, 2H), 3.74 (s, 3H), 2.46 (s, 3H). ^{13}C NMR (100 MHz, CD_3COCD_3): δ 146.0, 133.5, 130.9, 128.8, 57.0, 21.5. MS (ESI) m/z 187 ($\text{M} + \text{H}^+$, positive mode).

Methyl-*d*₃ 4-Methylbenzenesulfonate (33**).** Compound **33** (12.8 g, 68%) was prepared as a white solid from methanol-*d*₄ (3.61 g, 100 mmol, 99.5 atom % D) according to the method described for the synthesis of **29**. ^1H NMR (400 MHz, CD_3COCD_3): δ 7.80 (d, $J = 8.0$ Hz, 2H), 7.49 (d, $J = 8.0$ Hz, 2H), 2.46 (s, 3H). ^{13}C NMR (100 MHz, CD_3COCD_3): δ 145.9, 133.4, 130.9, 128.8, 21.5. MS (ESI) m/z 190 ($\text{M} + \text{H}^+$, positive mode).

(2*S*,3*R*,4*R*,5*S*,6*R*)-2-(4-Chloro-3-(4-(ethoxy-*d*₃)benzyl)phenyl)-6-(hydroxymethyl)tetrahydro-2*H*-pyran-3,4,5-triol (34**).** Compound **34** (82.7 mg, 76% yield, HPLC purity (condition I): 99.6%) was prepared as a white solid from **11** (100 mg, 0.263 mmol) and **30** (59.3 mg, 0.289 mmol) according to the method described for the synthesis of **5**. ^1H NMR (400 MHz, CD_3OD): δ 7.35–7.32 (m, 2H), 7.27 (d, $J = 8.4$ Hz, 1H), 7.09 (d, $J = 8.4$ Hz, 2H), 6.79 (d, $J = 8.4$ Hz, 2H), 4.10–3.97 (m, 3H), 3.87 (d, $J = 11.6$ Hz, 1H), 3.69 (dd, $J = 4.8, 11.6$ Hz, 1H), 3.47–3.43 (m, 1H), 3.42–3.35 (m, 2H), 3.29–3.26 (m, 1H). ^{13}C NMR (100 MHz, CD_3OD): δ 158.9, 140.0, 139.9, 134.4, 132.8, 131.9, 130.8, 130.1, 128.2, 115.4, 82.9, 82.2, 79.7, 76.5, 71.8, 63.1, 39.2. MS (ESI) m/z 431 ($\text{M} + \text{NH}_4^+$, positive mode), 458 ($\text{M} + \text{HCO}_2^-$, negative mode). HRMS: m/z calcd for $\text{C}_{21}\text{H}_{20}\text{D}_3\text{Cl}_2\text{O}_6$ ($\text{M} + \text{Cl}^-$) 448.1348; found, 448.1362.

(2*S*,3*R*,4*R*,5*S*,6*R*)-2-(4-Chloro-3-(4-(ethoxy-1,1-*d*₂)benzyl)phenyl)-6-(hydroxymethyl)tetrahydro-2*H*-pyran-3,4,5-triol (35**).** Compound **35** (77.8 g, 72% yield, HPLC purity (condition I): 99.6%) was prepared as a white solid from **11** (100 mg, 0.263 mmol) and

31 (58.5 mg, 0.289 mmol) according to the method described for the synthesis of **5**. ^1H NMR (400 MHz, CD_3OD): δ 7.35–7.32 (m, 2H), 7.27 (dd, $J = 1.6, 8.0$ Hz, 1H), 7.09 (d, $J = 8.8$ Hz, 2H), 6.79 (d, $J = 8.8$ Hz, 2H), 4.09 (d, $J = 9.2$ Hz, 1H), 4.05 (d, $J = 15.2$ Hz, 1H), 3.99 (d, $J = 15.2$ Hz, 1H), 3.87 (d, $J = 12.0$ Hz, 1H), 3.69 (dd, $J = 5.2, 12.0$ Hz, 1H), 3.48–3.44 (m, 1H), 3.43–3.37 (m, 2H), 3.30–3.26 (m, 1H), 1.33 (s, 3H). ^{13}C NMR (100 MHz, CD_3OD): δ 158.8, 140.0, 139.9, 134.4, 132.9, 131.9, 130.8, 130.1, 128.2, 115.4, 82.9, 82.2, 79.7, 76.4, 71.8, 63.1, 39.2, 14.9. MS (ESI) m/z 411 ($\text{M} + \text{H}^+$, positive mode), 455 ($\text{M} + \text{HCO}_2^-$, negative mode). HRMS: m/z calcd for $\text{C}_{21}\text{H}_{22}\text{D}_2\text{ClO}_6$ ($\text{M} - \text{H}^+$), 409.1393; found, 409.1406.

(2S,3R,4S,5S,6R)-2-(4-Chloro-3-(4-ethoxybenzyl)phenyl)-2-d-6-(hydroxymethyl)tetrahydro-2H-pyran-3,4,5-triol (36). Compound **36** (80.5 mg, 75% yield, HPLC purity (condition I): 99.7%) was prepared as a white solid from **25** (100 mg, 0.262 mmol) and **29** (57.7 mg, 0.288 mmol) according to the method described for the synthesis of **5**. ^1H NMR (400 MHz, CD_3OD): δ 7.35–7.32 (m, 2H), 7.27 (d, $J = 8.4$ Hz, 1H), 7.09 (d, $J = 8.4$ Hz, 2H), 6.79 (d, $J = 8.4$ Hz, 2H), 4.07–4.01 (m, 2H), 3.98 (q, $J = 7.2$ Hz, 2H), 3.87 (d, $J = 12.0$ Hz, 1H), 3.69 (dd, $J = 4.8, 12.0$ Hz, 1H), 3.48–3.43 (m, 1H), 3.42–3.35 (m, 2H), 3.29–3.26 (m, 1H), 1.35 (t, $J = 7.2$ Hz, 3H). ^{13}C NMR (100 MHz, CD_3OD): δ 158.8, 140.0, 139.9, 134.4, 132.9, 131.9, 130.8, 130.1, 128.2, 115.4, 82.2, 79.7, 76.4, 71.8, 64.4, 63.1, 39.2, 15.2. MS (ESI) m/z 410 ($\text{M} + \text{H}^+$, positive mode), 454 ($\text{M} + \text{HCO}_2^-$, negative mode). HRMS: m/z calcd for $\text{C}_{21}\text{H}_{24}\text{DCl}_2\text{O}_6$ ($\text{M} + \text{Cl}^-$), 444.1096; found, 444.1101.

(2S,3R,4R,5S,6R)-2-(4-Chloro-3-((4-ethoxyphenyl)methyl)-d₂-phenyl)-6-(hydroxymethyl)tetrahydro-2H-pyran-3,4,5-triol (37). Compound **37** (75.1 mg, 70% yield, HPLC purity (condition I): 99.0%) was prepared as a white solid from **26** (100 mg, 0.261 mmol) and **29** (57.5 mg, 0.287 mmol) according to the method described for the synthesis of **5**. ^1H NMR (400 MHz, CD_3OD): δ 7.35–7.32 (m, 2H), 7.27 (dd, $J = 2.4, 8.4$ Hz, 1H), 7.09 (d, $J = 8.8$ Hz, 2H), 6.79 (d, $J = 8.8$ Hz, 2H), 4.09 (d, $J = 9.6$ Hz, 1H), 3.99 (q, $J = 7.2$ Hz, 2H), 3.87 (d, $J = 11.6$ Hz, 1H), 3.69 (dd, $J = 5.2, 11.6$ Hz, 1H), 3.48–3.43 (m, 1H), 3.42–3.36 (m, 2H), 3.29–3.26 (m, 1H), 1.35 (t, $J = 7.2$ Hz, 3H). ^{13}C NMR (100 MHz, CD_3OD): δ 158.8, 140.0, 139.9, 134.4, 132.8, 131.9, 130.8, 130.1, 128.2, 115.4, 82.9, 82.2, 79.7, 76.4, 71.8, 64.4, 63.1, 15.2. MS (ESI) m/z 411 ($\text{M} + \text{H}^+$, positive mode), 455 ($\text{M} + \text{HCO}_2^-$, negative mode). HRMS: m/z calcd for $\text{C}_{21}\text{H}_{23}\text{D}_2\text{Cl}_2\text{O}_6$ ($\text{M} + \text{Cl}^-$), 445.1159; found, 445.1168.

(2S,3R,4R,5S,6R)-2-(4-Chloro-3-((4-(ethoxy-d₅)phenyl)methyl)-d₂phenyl)-6-(hydroxymethyl)tetrahydro-2H-pyran-3,4,5-triol (38). Compound **38** (73.8 mg, 68% yield, HPLC purity (condition I): 98.8%) was prepared as a white solid from **26** (100 mg, 0.261 mmol) and **30** (58.9 mg, 0.287 mmol) according to the method described for the synthesis of **5**. ^1H NMR (400 MHz, CD_3OD): δ 7.35–7.32 (m, 2H), 7.27 (dd, $J = 2.0, 8.0$ Hz, 1H), 7.09 (d, $J = 8.4$ Hz, 2H), 6.79 (d, $J = 8.4$ Hz, 2H), 3.87 (d, $J = 12.0$ Hz, 1H), 3.69 (dd, $J = 5.2, 12.0$ Hz, 1H), 3.47–3.43 (m, 1H), 3.42–3.35 (m, 2H), 3.29–3.26 (m, 1H). ^{13}C NMR (100 MHz, CD_3OD): δ 158.9, 140.0, 139.9, 134.4, 132.8, 131.9, 130.8, 130.1, 128.2, 115.4, 82.9, 82.2, 79.7, 76.5, 71.8, 63.1. MS (ESI) m/z 438 ($\text{M} + \text{Na}^+$, positive mode), 460 ($\text{M} + \text{HCO}_2^-$, negative mode). HRMS: m/z calcd for $\text{C}_{21}\text{H}_{18}\text{D}_7\text{ClNaO}_6$ ($\text{M} + \text{Na}^+$), 438.1671; found, 438.1676.

(2S,3R,4R,5S,6R)-2-(4-Chloro-3-((4-ethoxyphenyl)methyl)-d₂-phenyl)-2-d-6-(hydroxymethyl)tetrahydro-2H-pyran-3,4,5-triol (39). Compound **39** (78.5 mg, 73% yield, HPLC purity (condition I): 99.1%) was prepared as a white solid from **27** (100 mg, 0.261 mmol) and **29** (57.5 mg, 0.287 mmol) according to the method described for the synthesis of **5**. ^1H NMR (400 MHz, CD_3OD): δ 7.35–7.32 (m, 2H), 7.27 (dd, $J = 2.0, 8.4$ Hz, 1H), 7.09 (d, $J = 8.8$ Hz, 2H), 6.79 (d, $J = 8.8$ Hz, 2H), 4.09 (d, $J = 9.6$ Hz, 1H), 3.97 (q, $J = 6.8$ Hz, 2H), 3.87 (d, $J = 12.0$ Hz, 1H), 3.69 (dd, $J = 5.2, 12.0$ Hz, 1H), 3.48–3.44 (m, 1H), 3.43–3.35 (m, 2H), 3.30–3.27 (m, 1H), 1.35 (t, $J = 6.8$ Hz, 3H). ^{13}C NMR (100 MHz, CD_3OD): δ 158.9, 140.0, 139.9, 134.4, 132.9, 131.9, 130.8, 130.1, 128.2, 115.5, 82.2, 79.8, 76.4, 71.9, 64.5, 63.1, 15.2. MS (ESI) m/z 429 ($\text{M} + \text{NH}_4^+$, positive mode), 456 ($\text{M} + \text{HCO}_2^-$, negative mode). HRMS: m/z calcd for $\text{C}_{21}\text{H}_{21}\text{D}_3\text{ClO}_6$ ($\text{M} - \text{H}^+$), 410.1456; found, 410.1445.

(2S,3R,4R,5S,6R)-2-(4-Chloro-3-((4-(ethoxy-d₅)phenyl)methyl)-d₂phenyl)-2-d-6-(hydroxymethyl)tetrahydro-2H-

pyran-3,4,5-triol (40).⁵³ To a stirred solution of **27** (100 mg, 0.261 mmol) and **30** (58.9 mg, 0.287 mmol) in *N,N*-dimethylformamide (1.5 mL) was added cesium carbonate (258 mg, 0.79 mmol) followed by addition of tetrabutylammonium iodide (9.7 mg, 0.026 mmol). After stirring for 12 h at 40 °C under argon, the mixture was quenched by addition of ice water (10 mL). The mixture was extracted with ethyl acetate (2 × 20 mL). The combined organic layers were washed with water (20 mL) and brine (20 mL), dried over anhydrous sodium sulfate, and concentrated, and the residue was purified by preparative TLC to give product **40** (81.6 mg, 75% yield, HPLC purity (condition I): 99.9%) as a white solid. ^1H NMR (400 MHz, CD_3OD): δ 7.35–7.32 (m, 2H), 7.27 (dd, $J = 2.0, 8.4$ Hz, 1H), 7.09 (d, $J = 8.4$ Hz, 2H), 6.79 (d, $J = 8.4$ Hz, 2H), 4.09 (d, $J = 9.6$ Hz, 1H), 3.87 (d, $J = 12.4$ Hz, 1H), 3.69 (dd, $J = 4.8, 11.6$ Hz, 1H), 3.47–3.43 (m, 1H), 3.42–3.35 (m, 2H), 3.29–3.26 (m, 1H). ^{13}C NMR (100 MHz, CD_3OD): δ 158.9, 140.0, 139.9, 134.4, 132.8, 131.9, 130.8, 130.1, 128.2, 115.4, 82.2, 79.8, 76.4, 71.9, 63.1. MS (ESI) m/z 417 ($\text{M} + \text{H}^+$, positive mode), 461 ($\text{M} + \text{HCO}_2^-$, negative mode). HRMS: m/z calcd for $\text{C}_{21}\text{H}_{17}\text{D}_8\text{ClO}_6$ ($\text{M} - \text{H}^+$), 415.1842; found, 415.1769.

(2S,3R,4R,5S,6R)-2-(4-Chloro-3-(4-(methoxy-d₃)benzyl)phenyl)-6-(hydroxymethyl)tetrahydro-2H-pyran-3,4,5-triol (41). Compound **41** (75.3 mg, 72% yield, HPLC purity (condition I): 99.1%) was prepared as a white solid from **11** (100 mg, 0.263 mmol) and **33** (54.8 mg, 0.289 mmol) according to the method described for the synthesis of **5**. ^1H NMR (400 MHz, CD_3OD): δ 7.34 (d, $J = 8.0$ Hz, 1H), 7.32 (d, $J = 2.0$ Hz, 1H), 7.27 (dd, $J = 2.0, 8.0$ Hz, 1H), 7.10 (d, $J = 8.8$ Hz, 2H), 6.81 (d, $J = 8.8$ Hz, 2H), 4.10–3.98 (m, 3H), 3.87 (d, $J = 11.6$ Hz, 1H), 3.69 (dd, $J = 5.2, 11.6$ Hz, 1H), 3.48–3.43 (m, 1H), 3.42–3.35 (m, 2H), 3.30–3.27 (m, 1H). ^{13}C NMR (100 MHz, CD_3OD): δ 159.6, 140.0, 139.9, 134.4, 132.9, 131.9, 130.8, 130.1, 128.2, 114.8, 82.9, 82.2, 79.7, 76.5, 71.8, 63.1, 39.2. MS (ESI) m/z 415 ($\text{M} + \text{NH}_4^+$, positive mode), 442 ($\text{M} + \text{HCO}_2^-$, negative mode). HRMS: m/z calcd for $\text{C}_{20}\text{H}_{20}\text{D}_3\text{ClNaO}_6$ ($\text{M} + \text{Na}^+$), 420.1264; found, 420.1264.

(2S,3R,4R,5S,6R)-2-(4-Chloro-3-((4-(methoxy-d₃)phenyl)methyl)-d₂phenyl)-6-(hydroxymethyl)tetrahydro-2H-pyran-3,4,5-triol (42). Compound **42** (73.0 mg, 70% yield, HPLC purity (condition I): 99.6%) was prepared as a white solid from **26** (100 mg, 0.261 mmol) and **33** (54.3 mg, 0.287 mmol) according to the method described for the synthesis of **5**. ^1H NMR (400 MHz, CD_3OD): δ 7.35–7.32 (m, 2H), 7.27 (dd, $J = 2.0, 8.4$ Hz, 1H), 7.10 (d, $J = 8.8$ Hz, 2H), 6.80 (d, $J = 8.8$ Hz, 2H), 4.09 (d, $J = 9.6$ Hz, 1H), 3.87 (d, $J = 12.0$ Hz, 1H), 3.69 (dd, $J = 5.2, 12.0$ Hz, 1H), 3.48–3.43 (m, 1H), 3.42–3.36 (m, 2H), 3.30–3.27 (m, 1H). ^{13}C NMR (100 MHz, CD_3OD): δ 159.6, 140.0, 139.9, 134.4, 132.9, 131.9, 130.8, 130.1, 128.2, 114.8, 82.9, 82.2, 79.7, 76.4, 71.8, 63.1. MS (ESI) m/z 422 ($\text{M} + \text{Na}^+$, positive mode), 444 ($\text{M} + \text{HCO}_2^-$, negative mode). HRMS: m/z calcd for $\text{C}_{20}\text{H}_{18}\text{D}_5\text{ClNaO}_6$ ($\text{M} + \text{Na}^+$), 422.1389; found, 422.1382.

(2S,3R,4R,5S,6R)-2-(4-Chloro-3-((4-(methoxy-d₃)phenyl)methyl)-d₂phenyl)-2-d-6-(hydroxymethyl)tetrahydro-2H-pyran-3,4,5-triol (43). Compound **43** (75.3 mg, 72% yield, HPLC purity (condition I): 99.8%) was prepared as a white solid from **27** (100 mg, 0.261 mmol) and **33** (54.3 mg, 0.287 mmol) according to the method described for the synthesis of **5**. ^1H NMR (400 MHz, CD_3OD): δ 7.35–7.32 (m, 2H), 7.27 (dd, $J = 2.0, 8.0$ Hz, 1H), 7.11 (d, $J = 8.4$ Hz, 2H), 6.80 (d, $J = 8.4$ Hz, 2H), 3.87 (d, $J = 11.6$ Hz, 1H), 3.69 (dd, $J = 5.2, 11.6$ Hz, 1H), 3.48–3.43 (m, 1H), 3.42–3.35 (m, 2H), 3.30–3.27 (m, 1H). ^{13}C NMR (100 MHz, CD_3OD): δ 159.6, 140.0, 139.9, 134.5, 132.9, 131.9, 130.8, 130.1, 128.2, 114.8, 82.2, 79.8, 76.4, 71.9, 63.1. MS (ESI) m/z 418 ($\text{M} + \text{NH}_4^+$, positive mode), 444 ($\text{M} + \text{HCO}_2^-$, negative mode). HRMS: m/z calcd for $\text{C}_{20}\text{H}_{16}\text{D}_6\text{ClO}_6$ ($\text{M} - \text{H}^+$), 399.1488; found, 399.1475.

Glucose Uptake Inhibition Assay. A plasmid bearing the human full-length SGLT1 coding sequence in the pDream 2.1 mammalian expression vector was purchased from GenScript Corporation. Full-length human SGLT2 cDNA (GenScript Corporation) was cloned into the pEAK15 mammalian expression vector. Human SGLT1 expression plasmid DNA was transfected into COS-7 cells (American Type Culture Collection) using Lipofectamine 2000 (Invitrogen Corporation). Transfected cells were evaluated for SGLT1 activity in a methyl- α -D-[U- ^{14}C]glucopyranoside (AMG) uptake assay and cryopreserved until

use. The plasmid encoding human SGLT2 was linearized and stably transfected into 293.ETN cells. SGLT2-expressing clones were selected on the basis of resistance to puromycin (Invitrogen Corporation) and activity in the AMG uptake assay. CHO-K1 cells expressing SGLT1 or SGLT2 were seeded on 96-well ScintiPlates (PerkinElmer, Inc.) in DMEM containing 10% FBS (1×10^5 cells per well in 100 μ L of medium) incubated at 37 °C under 5% CO₂ for 48 h prior to the assay. Cells were washed twice with 150 μ L of either sodium buffer (137 mM NaCl, 5.4 mM KCl, 2.8 mM CaCl₂, 1.2 mM MgCl₂, 10 mM tris(hydroxymethyl)aminomethane/*N*-2-hydroxyethylpiperazine-*N'*-ethanesulfonic acid [Tris/Hepes], pH 7.2) or sodium-free buffer (137 mM *N*-methyl-glucamine, 5.4 mM KCl, 2.8 mM CaCl₂, 1.2 mM MgCl₂, 10 mM Tris/Hepes, pH 7.2). Test compound in 50 μ L each of sodium or sodium-free buffer containing 40 μ Ci/mL methyl- α -D-[U-¹⁴C]-glucopyranoside (Amersham Biosciences/GE Healthcare) and 25% human plasma was added per well of a 96-well plate and incubated at 37 °C with shaking for either 2 (SGLT1 assay) or 1.5 h (SGLT2 assay). Cells were washed twice with 150 μ L of wash buffer (137 mM *N*-methylglucamine, 10 mM Tris/Hepes, pH 7.2), and methyl- α -D-[U-¹⁴C]glucopyranoside uptake was quantitated using a TopCount scintillation counter (PerkinElmer, Inc.). Compounds were initially screened at three different concentrations in triplicate measurements. Potent and selective SGLT2 inhibitors were further evaluated at eight concentrations in triplicate. Sodium-dependent glucopyranoside uptake was calculated by subtracting the values obtained with sodium-free buffer from those obtained using sodium buffer. In general, ratios of sodium-dependent to sodium-independent AMG uptake in SGLT1- and SGLT2-expressing cells were 10–15 and 15–20, respectively. Results of AMG uptake were analyzed using GraphPad Prism (Intuitive Software for Science). IC₅₀ calculations were performed using nonlinear regression with variable slope. As a reference standard, (2*S*,3*R*,4*R*,5*S*,6*R*)-2-(4-chloro-3-(4-ethylbenzyl)phenyl)-6-(hydroxymethyl) tetrahydro-2*H*-pyran-3,4,5-triol was routinely included in the assays. In 26-independent evaluations, the reference compound inhibited SGLT2 activity by $69.7 \pm 9.6\%$ at 10 nM and SGLT1 by $72.7 \pm 6.7\%$ at 10 μ M.

Pharmacokinetic Parameters in SD Rats. Route of Administration: p.o. (IG) and i.v.

Collection Means. Three-hundred microliters of blood was collected from the orbital plexus into tubes after the animal was temporarily anesthetized by ether inhalation. The tubes were filled full for about 12 h with a saline solution containing heparin (1000 units/mL), the saline was removed, and the tubes were dried at 105 °C before use. At the last data point, animals were sacrificed by ether inhalation after the blood was collected. Animals were disposed of without further analysis.

Blood Samples. Immediately after collection, blood collection tubes were gently inverted at least five times, ensuring complete mixing, and were then immediately placed on ice. The blood was centrifuged for 5 min at 5000 rpm and 4 °C to separate the plasma from the red blood cells. After separation, 200 μ L disposable pipettes were used to take 100 μ L aliquots from the top plasma layer into tubes, with each being labeled by the name of analysis unit. Plasma was frozen on dry ice and stored at –80 °C until removal for LC–MS/MS analysis for the test compound concentration.

Each test compound was dissolved in 30% poly(ethylene glycol) (average molecular weight of 400, PEG400) and administered orally to overnight-fasted Sprague–Dawley rats ($n = 4$ per group) by gavage at the dose level of 3 mg/kg (or 1 mg/kg). Control rats were given 30% PEG400 only. One hour postdosing, a glucose solution (2 g/kg, 10 mL/kg) was administered by oral gavage. Each test compound was evaluated in four Sprague–Dawley (SD) rats following a single oral administration of 3 mg/kg (or 1 mg/kg) of the compound. The plasma samples were collected from the orbital plexus at 0.083, 0.25, 0.50, 1.0, 2.0, 4.0, 6.0, 8.0, 10, 12, and 24 h postdose, and the drug concentrations in the samples were determined using an established LC–MS/MS system after deproteinization. LC–MS/MS analysis was performed using a Dionex Ultimate 3000 HPLC system and an Applied Biosystems 4000 Q-Trap mass spectrometer with an ESI source. Chromatographic separation was achieved using a Kromasil C18 column (2.1 mm \times 150 mm, 5 μ m) (EKA Chemicals Co., Sweden). The mobile phase consisted of acetonitrile/10

mM ammonium formate solution (4:6, v/v), and the flow rate was set at 0.3 mL/min. The injection cycle of each sample was set at 10 min. Noncompartmental pharmacokinetic parameters were calculated on the basis of the plasma concentration–time data using WinNonlin Professional 5.0 (Pharsight, Mountain View, CA). The cumulative drug amount excreted into urine was divided by the corresponding AUC to estimate renal clearance.

Urinary Glucose Excretion in SD Rats. Each test compound was dissolved in 30% PEG400 and administered orally to overnight-fasted Sprague–Dawley rats ($n = 3$ per group) by gavage at the dose level of 1 mg/kg. Control rats were given 30% PEG400 only. One hour postdosing, a glucose solution (2 g/kg, 10 mL/kg) was administered by oral gavage. Urine was collected within metabolic cages from 0 to 4 and 4 to 24 h postdosing for urine volume and glucose measurement. Food was removed 16 h before dosing and then provided 3 h after dosing. Water was supplied ad libitum. The concentration of urinary glucose was determined at 4 and 24 h postdose using a biochemistry analyzer. Results were recorded for the periods 0–4, 4–24, and 0–24 h and expressed as a percentage of the urinary glucose excretion (UGE) seen with reference 5, which was run as a positive control in all experiments.

Urinary Glucose Excretion in Beagle Dogs. Each test compound was dissolved in 10% PEG400 and administered orally to overnight-fasted beagle dogs ($n = 3$ per group) by gavage at the dose level of 0.03 mg/kg. Control dogs were given 10% PEG400 only. One hour postdosing, a glucose solution (2 g/kg, 5 mL/kg) was administered by oral gavage. Urine was collected within metabolic cages from 0 to 8 and 8 to 24 h postdosing for urine volume and glucose measurement. Food was removed 16 h before dosing and then provided 3 h after dosing. Water was supplied ad libitum. The concentration of urinary glucose was determined at 8 and 24 h postdose using a biochemistry analyzer. Results were recorded for the periods 0–8, 8–24, and 0–24 h and expressed as a percentage of the urinary glucose excretion (UGE) seen with reference 5, which was run as a positive control in all experiments.

Urinary Glucose Excretion and Oral Glucose-Tolerance Test in SD Rats. Compound 41 was administered orally to overnight-fasted Sprague–Dawley rats ($n = 5$ per group) by gavage at different doses (0.1, 0.3, 1, 3, and 10 mg/kg). Control rats were given the vehicle of 30% PEG400 only. One hour postdosing, a glucose solution (2 g/kg, 10 mL/kg) was administered by oral gavage. Blood glucose concentration was measured before dosing, before the glucose challenge, and 15, 30, 60, and 120 min after glucose challenge. Urine was collected from 0 to 4, 4 to 8, and 8 to 24 h postdosing for glucose measurement. Urine volumes and food and water consumption were also recorded. Blood glucose levels were determined using a glucometer (One Touch, LifeScan Inc.). The glucose concentration in urine was determined using a Hitachi 7080 automatic biochemistry analyzer.

■ ASSOCIATED CONTENT

📄 Supporting Information

HPLC-MS chromatographic metabolic monitoring for 41, metabolic process confirmation for 41 and 5 by HPLC-MS chromatography, and ¹H and ¹³C NMR spectra for all new compounds. This material is available free of charge via the Internet at <http://pubs.acs.org>.

■ AUTHOR INFORMATION

Corresponding Author

*Tel: +86 21 51980003. Fax: +86 21 51980003. E-mail: sunxunf@shmu.edu.cn.

Notes

The authors declare no competing financial interest.

■ ACKNOWLEDGMENTS

Financial support from the Shanghai Municipal Committee of Science and Technology (no. 10431903100) and the National Basic Research Program of China (973 Program, no.

2010CB912603) are acknowledged. We also thank the analytical group of Egret Pharma (Shanghai) Limited for providing analytical service.

■ ABBREVIATIONS USED

SGLT, sodium-dependent glucose cotransporter; UGE, urinary glucose excretion; WHO, World Health Organization; DM2, type 2 diabetes mellitus; FDA, U.S. Food and Drug Administration; EMA, European Medicines Agency; ADME, absorption, distribution, metabolism, and excretion; PK, pharmacokinetics; AUC, area under the plasma concentration time curve; *F*, oral bioavailability; *IC*₅₀, half-maximal inhibitory concentration; THF, tetrahydrofuran; TBDMS, tertbutyldimethylsilyl; DMF, *N,N*-dimethylformamide; PEG400, poly(ethylene glycol) (average molecular weight of 400)

■ REFERENCES

- (1) World Health Organization diabetes fact sheet (no. 312). <http://www.who.int/mediacentre/factsheets/fs312> (accessed August 2013).
- (2) Facchini, F. S.; Hua, N.; Abbasi, F.; Reaven, G. M. Insulin resistance as a predictor of age-related diseases. *J. Clin. Endocrinol. Metab.* **2001**, *86*, 3574–3578.
- (3) Stumvoll, M.; Goldstein, B. J.; van Haeften, T. W. Type 2 diabetes: Principles of pathogenesis and therapy. *Lancet* **2005**, *365*, 1333–1346.
- (4) Davidson, M. B.; Peters, A. L. An overview of metformin in the treatment of type 2 diabetes mellitus. *Am. J. Med.* **1997**, *102*, 99–110.
- (5) Horii, S.; Fukase, H.; Matsuo, T.; Kameda, Y.; Asano, N.; Matsui, K. Synthesis and R-D-glucosidase inhibitory activity of N-substituted valiolamine derivatives as potential oral antidiabetic agents. *J. Med. Chem.* **1986**, *29*, 1038–1046.
- (6) Davis, S. N. The role of glimepiride in the effective management of type 2 diabetes. *J. Diabetes Complications* **2004**, *18*, 367–376.
- (7) Marco, S.; Michael, P.; Adrian, R.; Hubert, H.; Sander, K.; Hugo, A.; Torsten, S.; Urs, A. M.; Christoph, R. Sulfonylureas and glinides exhibit peroxisome proliferator-activated receptor γ activity: A combined virtual screening and biological assay approach. *Mol. Pharmacol.* **2007**, *71*, 398–406.
- (8) Ajjan, R. A.; Grant, P. J. The cardiovascular safety of rosiglitazone. *Expert Opin. Drug Saf.* **2008**, *7*, 367–376.
- (9) Momose, Y.; Meguro, K.; Ikeda, H.; Hatanaka, C.; Oi, S.; Shoda, T. Studies on antidiabetic agents. X. Synthesis and biological activities of pioglitazone and related compounds. *Chem. Pharm. Bull.* **1991**, *39*, 1440–1445.
- (10) Kim, D.; Wang, L.; Beconi, M.; Eiermann, G. J.; Fisher, M. H.; He, H.; Hickey, G. J.; Kowalchick, J. E.; Leiting, B.; Lyons, K.; Marsilio, F.; McCann, M. E.; Patel, R. A.; Petrov, A.; Scapin, G.; Patel, S. B.; Roy, R. S.; Wu, J. K.; Wyvratt, M. J.; Zhang, B. B.; Zhu, L.; Thornberry, N. A.; Weber, A. E. (2R)-4-Oxo-4-[3-(trifluoromethyl)-5,6-dihydro[1,2,4]-triazolo[4,3-R]pyrazin-7(8H)-yl]-1-(2,4,5-trifluorophenyl)butan-2-amine: A potent, orally active dipeptidyl peptidase IV inhibitor for the treatment of type 2 diabetes. *J. Med. Chem.* **2005**, *48*, 141–151.
- (11) Dicker, D. DPP-4 inhibitors. Impact on glycemic control and cardiovascular risk factors. *Diabetes Care* **2011**, *34*, S276–S278.
- (12) Vallon, V.; Platt, K. A.; Cunard, R.; Schroth, J.; Whaley, J.; Thomson, S. C.; Koepsell, H.; Rieg, T. SGLT2 mediates glucose reabsorption in the early proximal tubule. *J. Am. Soc. Nephrol.* **2011**, *22*, 104–112.
- (13) Kanai, Y.; Lee, W.-S.; You, G.; Brown, D.; Hediger, M. A. The human kidney low affinity Na⁺/glucose cotransporter SGLT2. Delineation of the major renal reabsorptive mechanism for D-glucose. *J. Clin. Invest.* **1994**, *93*, 397–404.
- (14) Powell, D. R.; DaCosta, C. M.; Gay, J.; Ding, Z. M.; Smith, M.; Greer, J.; Doree, D.; Jeter-Jones, S.; Mseeh, F.; Rodriguez, L. A.; Harris, A.; Buhning, L.; Platt, K. A.; Vogel, P.; Brommage, R.; Shadoan, M. K.; Sands, A. T.; Zambrowicz, B. Improved glycemic control in mice lacking Sglt1 and Sglt2. *Am. J. Physiol.: Endocrinol. Metab.* **2013**, *304*, E117–E130.
- (15) Chao, E. C.; Henry, R. R. SGLT2 inhibition—a novel strategy for diabetes treatment. *Nat. Rev. Drug Discovery* **2010**, *9*, 551–559.
- (16) Toggenburger, G.; Kessler, M.; Semenza, G. Phlorizin as a probe of the small-intestinal Na⁺, D-glucose cotransporter. A model. *Biochim. Biophys. Acta* **1982**, *688*, 557–571.
- (17) Ehrenkranz, J. R.; Lewis, N. G.; Kahn, C. R.; Roth, J. Phlorizin: A review. *Diabetes/Metab. Res. Rev.* **2005**, *21*, 31–38.
- (18) Oku, A.; Ueta, K.; Arakawa, K.; Ishihara, T.; Nawano, M.; Kuronuma, Y.; Matsumoto, M.; Saito, A.; Tsujihara, K.; Anai, M.; Asano, T.; Kanai, Y.; Endou, H. T-1095, an inhibitor of renal Na⁺-glucose cotransporters, may provide a novel approach to treating diabetes. *Diabetes* **1999**, *48*, 1794–1800.
- (19) Tsujihara, K.; Hongu, M.; Saito, K.; Kawanishi, H.; Kuriyama, K.; Matsumoto, M.; Oku, A.; Ueta, K.; Tsuda, M.; Saito, A. Na⁺-glucose cotransporter (SGLT) inhibitors as antidiabetic agents. 4. Synthesis and pharmacological properties of 4'-dehydroxyphlorizin derivatives substituted on the B ring. *J. Med. Chem.* **1999**, *42*, 5311–5324.
- (20) Katsuno, K.; Fujimori, Y.; Takemura, Y.; Hiratochi, M.; Itoh, F.; Komatsu, Y.; Fujikura, H.; Isaji, M. Sergliflozin, a novel selective inhibitor of low-affinity sodium glucose cotransporter (SGLT2), validates the critical role of SGLT2 in renal glucose reabsorption and modulates plasma glucose level. *J. Pharmacol. Exp. Ther.* **2007**, *320*, 323–330.
- (21) Fujimori, Y.; Katsuno, K.; Nakashima, I.; Ishikawa-Takemura, Y.; Fujikura, H.; Isaji, M. Remogliflozin etabonate, in a novel category of selective low-affinity sodium glucose cotransporter (SGLT2) inhibitors, exhibits antidiabetic efficacy in rodent models. *J. Pharmacol. Exp. Ther.* **2008**, *327*, 268–276.
- (22) Meng, W.; Ellsworth, B. A.; Nirschl, A. A.; McCann, P. J.; Patel, M.; Girotra, R. N.; Wu, G.; Sher, P. M.; Morrison, E. P.; Biller, S. A.; Zahler, R.; Deshpande, P. P.; Pullockaran, A.; Hagan, D. L.; Morgan, N.; Taylor, J. R.; Obermeier, M. T.; Humphreys, W. G.; Khanna, A.; Discenza, L.; Robertson, J. G.; Wang, A.; Han, S.; Wetterau, J. R.; Janovitz, E. B.; Flint, O. P.; Whaley, J. M.; Washburn, W. N. Discovery of dapagliflozin: A potent, selective renal sodium-dependent glucose cotransporter 2 (SGLT2) inhibitor for the treatment of type 2 diabetes. *J. Med. Chem.* **2008**, *51*, 1145–1149.
- (23) Nomura, S.; Sakamaki, S.; Hongu, M.; Kawanishi, E.; Koga, Y.; Sakamoto, T.; Yamamoto, Y.; Ueta, K.; Kimata, H.; Nakayama, K.; Tsuda-Tsukimoto, M. Discovery of canagliflozin, a novel C-glucoside with thiophene ring, as sodium-dependent glucose cotransporter 2 inhibitor for the treatment of type 2 diabetes mellitus. *J. Med. Chem.* **2010**, *53*, 6355–6360.
- (24) Imamura, M.; Nakanishi, K.; Suzuki, T.; Ikegai, K.; Shiraki, R.; Ogiyama, T.; Murakami, T.; Kurosaki, E.; Noda, A.; Kobayashi, Y.; Yokota, M.; Koide, T.; Kosakai, K.; Ohkura, Y.; Takeuchi, M.; Tomiyama, H.; Ohta, M. Discovery of ipragliflozin (ASP1941): A novel C-glucoside with benzothiophene structure as a potent and selective sodium glucose co-transporter 2 (SGLT2) inhibitor for the treatment of type 2 diabetes mellitus. *Bioorg. Med. Chem.* **2012**, *20*, 3263–3279.
- (25) Goodwin, N. C.; Mabon, R.; Harrison, B. A.; Shadoan, M. K.; Almstead, Z. Y.; Xie, Y.; Healy, J.; Buhning, L. M.; DaCosta, C. M.; Bardenhagen, J.; Mseeh, F.; Liu, Q.; Nouraldeen, A.; Wilson, A. G. E.; Kimball, S. D.; Powell, D. R.; Rawlins, D. B. Novel L-xylose derivatives as selective sodium-dependent glucose cotransporter 2 (SGLT2) inhibitors for the treatment of type 2 diabetes. *J. Med. Chem.* **2009**, *52*, 6201–6204.
- (26) Mascitti, V.; Maurer, T. S.; Robinson, R. P.; Bian, J.; Boustany-Kari, C. M.; Brandt, T.; Collman, B. M.; Kalgutkar, A. S.; Klenotic, M. K.; Leininger, M. T.; Lowe, A.; Maguire, R. J.; Masterson, V. M.; Miao, Z.; Mukaiyama, E.; Patel, J. D.; Pettersen, J. C.; Prévile, C.; Samas, B.; She, L.; Sobol, Z.; Stepan, C. M.; Stevens, B. D.; Thuma, B. A.; Tugnait, M.; Zeng, D.; Zhu, T. Discovery of a clinical candidate from the structurally unique dioxo-bicyclo[3.2.1]octane class of sodium-dependent glucose cotransporter 2 inhibitors. *J. Med. Chem.* **2011**, *54*, 2952–2960.
- (27) Zhang, W.; Welihinda, A.; Mechanic, J.; Ding, H.; Zhu, L.; Lu, Y.; Deng, Z.; Sheng, Z.; Lv, B.; Chen, Y.; Roberge, J. Y.; Seed, B.; Wang, Y. EGT1442, a potent and selective SGLT2 inhibitor, attenuates blood

glucose and HbA1c levels in db/db mice and prolongs the survival of stroke-prone rats. *Pharmacol. Res.* **2011**, *63*, 284–293.

(28) Cai, M.; Liu, Q.; Xu, G.; Lv, B.; Seed, B.; Roberge, J. Y. Crystalline form of benzylbenzene SGLT2 inhibitor. PCT Int. Appl. WO2011153953, 2011.

(29) Mayer, P. Chances and risks of SGLT2 inhibitors. *Naunyn-Schmiedeberg's Arch. Pharmacol.* **2011**, 1–4.

(30) Dahl, S. G. Active metabolites of neuroleptic drugs: possible contribution to therapeutic and toxic effects. *Ther. Drug Monit.* **1982**, *4*, 33–40.

(31) Rogan, E. G.; Badawi, A. F.; Devanesan, P. D.; Meza, J. L.; Edney, J. A.; West, W. W.; Higginbotham, S. M.; Cavalieri, E. L. Relative imbalances in estrogen metabolism and conjugation in breast tissue of women with carcinoma: Potential biomarkers of susceptibility to cancer. *Carcinogenesis* **2003**, *24*, 697–702.

(32) Wu, Y.; Davis, C. D.; Dworetzky, S.; Fitzpatrick, W. C.; Harden, D.; He, H.; Knox, R. J.; Newton, A. E.; Philip, T.; Polson, C.; Sivarao, D. V.; Sun, L.; Tertyshnikova, S.; Weaver, D.; Yeola, S.; Zoeckler, M.; Sinz, M. W. Fluorine substitution can block CYP3A4 metabolism-dependent inhibition: Identification of (S)-N-[1-(4-fluoro-3-morpholin-4-ylphenyl)ethyl]-3-(4-fluorophenyl)acrylamide as an orally bioavailable KCNQ2 opener devoid of CYP3A4 metabolism-dependent inhibition. *J. Med. Chem.* **2003**, *46*, 3778–3781.

(33) Benz, C. C.; Atsriku, C.; Yau, C.; Britton, D.; Schilling, B.; Gibson, B. W.; Baldwin, M. A.; Scott, G. K. Novel pathways associated with quinone-induced stress in breast cancer cells. *Drug Metab. Rev.* **2006**, *38*, 601–613.

(34) Yao, M.; Cao, K.; Zhang, D.; Rodrigues, D.; Humphreys, W. G.; Zhu, M. Identification of the human UDP-glucuronosyltransferase enzymes involved in glucuronidation of dapagliflozin. American Association of Pharmaceutical Scientists Annual Meeting, Los Angeles, CA, November 8–12, 2009; T3130.

(35) Obermeier, M.; Yao, M.; Khanna, A.; Koplowitz, B.; Zhu, M.; Li, W.; Komoroski, B.; Kasichayanula, S.; Discenza, L.; Washburn, W.; Meng, W.; Ellsworth, B. A.; Whaley, J. M.; Humphreys, W. G. In vitro characterization and pharmacokinetics of dapagliflozin (BMS-512148), a potent sodium-glucose cotransporter type II (SGLT2) inhibitor, in animals and humans. *Drug Metab. Dispos.* **2010**, *38*, 405–414.

(36) Meanwell, N. A. Synopsis of some recent tactical application of bioisosteres in drug design. *J. Med. Chem.* **2011**, *54*, 2529–2591.

(37) Maltais, F.; Jung, Y. C.; Chen, M.; Tanoury, J.; Perni, R. B.; Mani, N.; Laitinen, L.; Huang, H.; Liao, S.; Gao, H.; Tsao, H.; Block, E.; Ma, C.; Shawgo, R. S.; Town, C.; Brummel, C. L.; Howe, D.; Pazhanisamy, S.; Raybuck, S.; Namchuk, M.; Bennani, Y. L. In vitro and in vivo isotope effects with hepatitis C protease inhibitors: Enhanced plasma exposure of deuterated telaprevir versus telaprevir in rats. *J. Med. Chem.* **2011**, *52*, 4993–8001.

(38) Sanderson, K. Big interest in heavy drugs. *Nature* **2009**, *458*, 269.

(39) Yarnell, A. T. Heavy-hydrogen drugs turn heads, again. Firms seek to improve drug candidates by selective deuterium substitution. *Chem. Eng. News* **2009**, *87*, 36–39.

(40) Schneider, F.; Hillgenberg, M.; Koytchev, R.; Alken, R.-G. Enhanced plasma concentration by selective deuteration of rofecoxib in rats. *Arzneim. Forsch.* **2006**, *56*, 295–300.

(41) Buteau, K. C. Deuterated drugs: Unexpectedly nonobvious? *J. High Tech. Law* **2009**, 22–74.

(42) Seed, B.; Lv, B.; Roberge, J. Y.; Chen, Y.; Peng, K.; Dong, J.; Xu, B.; Du, J.; Zhang, L.; Tang, X.; Xu, G.; Feng, Y.; Xu, M. Deuterated benzylbenzene derivatives and methods of use. PCT Int. Appl. WO2010009243, 2011.

(43) Smonou, I. One step reduction of diaryl ketones to hydrocarbons by etherated boron trifluoride-triethylsilane system. *Synth. Commun.* **1994**, *24*, 1999–2002.

(44) Nordlander, J. E.; Payne, M. J.; Njoroge, F.; Balk, M. A.; Laikos, G. D.; Vishwanath, V. M. Friedel–Crafts acylation with N-(trifluoroacetyl)-Cu-amino acid chlorides. Application to the preparation of β -arylalkylamines and 3-substituted 1,2,3,4-tetrahydroisoquinolines. *J. Org. Chem.* **1984**, *49*, 4107–4111.

(45) Davis, F. A.; Clark, C.; Kumar, A.; Chen, B.-C. Asymmetric synthesis of the AB ring segments of daunomycin and 4-demethoxydaunomycin. *J. Org. Chem.* **1994**, *59*, 1184–1190.

(46) Sandanayaka, V.; Mamat, B.; Mishra, R. K.; Winger, J.; Krohn, M.; Zhou, L.; Keyvan, M.; Enache, L.; Sullins, D.; Onua, E.; Zhang, J.; Halldorsdottir, G.; Sigthorsdottir, H.; Thorlaksdottir, A.; Sigthorsson, G.; Thorsteinnsson, M.; Davies, D. R.; Stewart, L. J.; Zembower, D. E.; Andresson, T.; Kiselyov, A. S.; Singh, J.; Gurney, M. E. Discovery of 4-[(2S)-2-{[4-(4-chlorophenoxy)phenoxy]methyl}-1-pyrrolidinyl]-butanoic acid (DG-051) as a novel leukotriene A4 hydrolase inhibitor of leukotriene B4 biosynthesis. *J. Med. Chem.* **2010**, *53*, 573–585.

(47) Guthikonda, R. N.; Cama, L. D.; Quesada, M.; Woods, M. F.; Salzmann, T. N.; Christensen, B. G. Structure–activity relationships in the 2-arylcarbapenem series: Synthesis of 1-methyl-2-arylcarbapenems. *J. Med. Chem.* **1987**, *30*, 871–880.

(48) Horton, D.; Priebe, W. Synthetic routes to higher-carbon sugars. Reaction of lactones with 2-lithio-1,3-dithiane. *Carbohydr. Res.* **1981**, *94*, 27–41.

(49) Czernecki, S.; Ville, G. C-glycosides. 7. Stereospecific C-glycosylation of aromatic and heterocyclic rings. *J. Org. Chem.* **1989**, *54*, 610–612.

(50) Kraus, G. A.; Molina, M. T. A direct synthesis of C-glycosyl compounds. *J. Org. Chem.* **1988**, *53*, 752–753.

(51) Yang, G.; Franck, R. W.; Byun, H.-S.; Bittman, R.; Samadder, P.; Arthur, G. Convergent C-glycolipid synthesis via the Ramberg–Bäcklund reaction: Active antiproliferative glycolipids. *Org. Lett.* **1999**, *1*, 2149–2151.

(52) Oikawa, H.; Suzuki, Y.; Katayama, K.; Naya, A.; Sakano, C.; Ichihara, A. Involvement of Diels–Alder reactions in the biosynthesis of secondary natural products: The late stage of the biosynthesis of the phytotoxins solanapyrones. *J. Chem. Soc., Perkin Trans. 1* **1999**, 1225–1232.

(53) Peng, X.; Lu, H.; Han, T.; Chen, C. Synthesis of a novel triptycene-based molecular tweezer and its complexation with paraquat derivatives. *Org. Lett.* **2007**, *9*, 895–898.

(54) The published in vitro data for dapagliflozin **5** give an EC₅₀ value of 1.1 nM for SGLT2 and a selectivity (*hSGLT1/hSGLT2*) of 1200-fold (ref 22). However, in our assays, we observed a 3.2 nM IC₅₀ value and 981-fold selectivity for *hSGLT2*.